

Photoinduced Electron Transfer Reactions of Aryl Olefins. 2.[†] Cis–Trans Isomerization and Cycloadduct Formation in Anethole–Fumaronitrile Systems in Polar Solvents

Martin Goez* and Gerd Eckert

Contribution from the Institut für Physikalische und Theoretische Chemie, Technische Universität Braunschweig, Hans-Sommer-Strasse 10, D-38106 Braunschweig, FRG

Received April 10, 1995[⊗]

Abstract: In acetonitrile, the photoreactions of *cis*-anethole, *cA*, or *trans*-anethole, *tA*, with fumarodinitrile, **FN**, lead to isomerization of both substrate and quencher and to mixed [2 + 2] cycloaddition. By NMR analysis and by NOE measurements it was shown that the same four stereoisomers of 1-anisyl-2-methyl-3,4-dicyanocyclobutane are formed in equal yields regardless of whether the substrate is *cA* or *tA*. The configuration of the anethole-derived moiety in these adducts is always *trans*, whereas all possible configurations of the cyano groups occur. From Stern–Volmer experiments it was concluded that the quenching mechanism is electron transfer, not exciplex formation. Electron-transfer quenching is also the pathway leading to the cycloadducts, as was established by photoinduced electron-transfer sensitization. These photoreactions give rise to strong nuclear spin polarizations (CIDNP) in the starting and isomerized forms of both substrate and quencher as well as in the cycloadducts. Radical pairs **A^{•+}FN^{•-}** (RP I) consisting of the radical cation of the anethole and the radical anion of fumarodinitrile were identified as the predominant source of the polarizations. The starting materials are regenerated by back electron transfer of singlet pairs; likewise, back electron transfer of triplet pairs ³RP I to give either triplet anethole, ³**A**, or triplet fumarodinitrile, ³**FN**, occurs and constitutes the main pathway to isomerization of substrate and quencher. The cycloadducts are also formed via ³RP I; a significant participation of free radicals in their generation was ruled out. The stereochemistry of the products and the different ratios of polarization intensities of the isomerized olefin and the cycloadducts can only be explained by the intermediacy of a triplet biradical ³**BR**. After intersystem crossing to the singlet state, ring closure of ¹**BR** competes with biradical scission. The latter process provides an additional isomerization pathway, which differs from the pathway via triplet olefins by leading only to one-way *cis*–*trans* isomerization of the substrate. ³**BR** is formed by geminate combination of triplet radical ion pairs ³RP I; an indirect pathway via back electron transfer of ³RP I to give ³**A** or ³**FN** followed by attack to the other olefin, as has been proposed for similar photocycloadditions, could be excluded unambiguously. Despite the different precursor multiplicity, the mechanism of the [2 + 2] photocycloaddition of donor and acceptor olefins investigated in this work is thus identical to the mechanism of the Paterno–Büchi reaction between donor olefins and electron-deficient carbonyl compounds which we recently reported. The CIDNP experiments at variable quencher concentration revealed the presence of an additional radical pair RP II, also containing **A^{•+}** but an anion other than **FN^{•-}**. It was shown that RP II results from a biphotonic process. These findings were explained by two-photon ionization of the anethole and formation of an oligomeric anion of acetonitrile.

The rapid development of organic photochemistry since the turn of the century is intimately linked with chemical transformations of olefins that are induced by visible or UV radiation, the gamut of classical reactions¹ ranging from the photodimerizations of cinnamic acid² and of stilbene³ to the synthesis of ascaridol on a technical scale by photooxygenation of α -terpinene.⁴ Within the broad spectrum of today's photochemical standard methods, reactions of olefins again occupy a central position, two outstanding representatives being the Paterno–Büchi reaction⁵ and photocycloadditions of enones to olefins.^{5b,6} Yet, from a more general, and less application-oriented, perspective natural processes involving olefins are of far greater

importance still. Photosynthesis and the mechanism of vision rely on the photophysical and photochemical properties of molecules containing conjugated double bonds. As a final example we mention the UV-induced [2 + 2] cycloaddition of thymine,⁷ which may cause irreversible, and often cancerogenic, damage to DNA.⁸

It is thus not surprising that olefin reactions have received considerable attention, [2 + 2] cycloadditions in particular belonging to the most intensively studied processes.^{9,10} Only in recent years has the intriguing fact been noted that the amount of charge separation during mixed cycloadditions of donor and acceptor olefins strongly influences the product distribution:

[†] Preceding paper in this series: see ref 17.

* Author to whom correspondence should be addressed.

[⊗] Abstract published in *Advance ACS Abstracts*, December 1, 1995.

(1) Roth, H. D. *Angew. Chem., Int. Ed. Engl.* **1989**, *28*, 1193–1207.

(2) Bertram, J.; Kürsten, R. *J. Prakt. Chem.* **1895**, *51*, 316–325.

(3) Ciamician, G.; Silber, P. *Chem. Ber.* **1902**, *35*, 4128–4131.

(4) (a) Schenck, G. O.; Ziegler, K. *Naturwissenschaften* **1944**, *32*, 157–157. (b) Schenck, G. O. *Angew. Chem.* **1952**, *64*, 12–23.

(5) See, for instance: (a) Jones, G. In *Organic Photochemistry*, Padwa, A., Ed.; Marcel Dekker: New York, 1981; Vol. 5, pp 1–122. (b) Demuth, M.; Mikhail, G. *Synthesis* **1989**, 145–162, and references therein.

(6) (a) Corey, E. J.; Bass, J. D.; LeMahieu, R.; Mitra, R. B. *J. Am. Chem. Soc.* **1964**, *86*, 5570–5583. (b) deMayo, P. *Acc. Chem. Res.* **1971**, *4*, 41–47. (c) Crimmins, M. T. *Chem. Rev.* **1988**, *88*, 1453–1473. (d) Schuster, D. I.; Lem, G.; Kaprinidis, N. A. *Chem. Rev.* **1993**, *93*, 3–22.

(7) Blackburn, G. M.; Davies, R. J. H. *J. Chem. Soc. (C)* **1966**, 2239–2244.

(8) Stryer, L. *Biochemistry*; Freeman: New York, 1988.

(9) Lewis, F. D. In *Photoinduced Electron Transfer. Part C. Organic Substrates*; Fox, M. A., Chanon, M., Eds.; Elsevier: New York, 1988; pp 1–69, and references therein.

(10) Mueller, F.; Mattay, J. *Chem. Rev.* **1993**, *93*, 99–117.

Often, quite different regioselectivities, stereoselectivities, periselectivities, and adduct yields are observed when only partial charge transfer occurs, i.e., when exciplexes are involved as polar intermediates, than under conditions leading to full charge separation, i.e., formation of radical ions.¹⁰ While the reactions of the former category have been extensively investigated,^{9,11} much less is known about the mechanisms of reactions falling into the latter category.⁹ From sensitization and scavenging studies as well as from energetic considerations it was concluded that in polar solvents the [2 + 2] cycloadditions of 1,2,3-triphenylcyclopropene with electron-deficient olefins such as fumarodinitrile¹² and the conceptually related [4 + 2] cycloaddition of a similar cyclopropene with dicyanoanthracene¹³ proceed by an electron-transfer/triplet mechanism: A radical ion pair is formed initially; this undergoes back electron transfer to give an olefin triplet (the cyclopropene triplet in these systems); attack by this species on the other olefin yields a triplet biradical which finally leads to the cycloadducts. As the primary excited species has singlet multiplicity in these reactions, intersystem crossing occurring in the radical ion pairs is therefore one of the key steps of this mechanism.

It is well known that in a magnetic field the rates of intersystem crossing in radical pairs are modulated by the hyperfine interactions with the nuclear spins, which leads to nonequilibrium populations of the nuclear spin states in the singlet and triplet pairs.¹⁴ By ensuing chemical reactions, these nuclear spin polarizations are ultimately transferred to diamagnetic products, where they manifest themselves as anomalous NMR line intensities. This effect, chemically induced dynamic nuclear polarization (CIDNP),¹⁴ thus appeared a convenient means to study such cycloadditions. Other attractive features of this method include the possibilities: first, to characterize both the products and the intermediates, the former being observed directly by high resolution NMR spectroscopy and the latter indirectly, because the relative polarization intensities of the different protons contain similar information as the EPR spectrum of the radicals composing the pairs;¹⁵ second, to determine the electron spin multiplicities of the species preceding the pairs and of the successor species formed via the different decay channels of the pairs, since the polarization phases depend on both; third, to separate in-cage reactions and reactions of escaping radicals by time-resolved experiments;¹⁶ and, finally, to trace the pathways from the intermediates to the products, because the polarizations are generated and detected at different stages of the reaction.

In this work, we therefore apply CIDNP techniques to the study of [2 + 2] photocycloadditions of donor olefins (*cis*- and *trans*-anethole) with an acceptor olefin (fumarodinitrile) in polar medium, mainly in acetonitrile. The energetics of these systems

Table 1. Pertinent Photophysical and Photochemical Data of *cis*- and *trans*-Anethole at Room Temperature

anethole	τ_0^S [ns]	k_q [$M^{-1} s^{-1}$]	k_M [$M^{-1} s^{-1}$] ^a	Φ_{iso} ^a
<i>trans</i>	8.5 ^{b,c}	3.0×10^{10}	3.2×10^8	0.12
<i>cis</i>	6.1 ^c	4.3×10^{10}	8.0×10^7	0.06

^a Reference 18b, in acetonitrile. ^b This work, in acetonitrile. The fluorescence decay was found to be monoexponential. ^c Reference 18b, in hexane.

are comparable to the above-mentioned examples: full charge separation is favored thermodynamically, and electron return of the radical ion pairs to give triplet olefins is also feasible. We present evidence that radical ion pairs are indeed formed and that they undergo intersystem crossing and react to triplet olefins. However, while the latter species provide the main pathway for geometric isomerization of the starting materials, cycloaddition does not proceed via this route but by geminate combination of triplet pairs to give triplet biradicals in a direct reaction. This is the same mechanism that we have previously found for the Paterno–Büchi reaction of these anetholes with quinones in acetonitrile.¹⁷

Results

Photophysics, Quenching Experiments, and Thermodynamics. The quencher fumarodinitrile, **FN**, does not display any measurable UV/vis absorption above 250 nm in the solvent used in this work, acetonitrile. When **FN** was added in high concentration (0.1 M) to a dilute solution (5×10^{-3} M) of *trans*-anethole, **tA**, a weak new absorption band was observed in the range of 310–370 nm indicating formation of a ground-state complex. However, even at 315 nm the absorbance of this complex did not amount to more than 5% of that of **tA**; below 310 nm it was undetectable and totally obscured by the latter. Selective excitation of the substrate **tA** is thus ensured in the fluorescence studies of this section ($\lambda_{exc} = 303$ nm) as well as in the photo-CIDNP experiments described below ($\lambda_{exc} = 308$ nm). A similar result is found with *cis*-anethole, **cA**, but in this case the relative absorbance of the complex is noticeably higher, about 13% of that of **cA** at 308 nm for the concentrations given. However, under typical conditions of our CIDNP measurements ($c(\mathbf{cA}) = 0.02$ M, $c(\mathbf{FN}) \leq 0.03$ M) excitation of the ground-state complex can also be neglected.

In acetonitrile, both **tA** and **cA** possess unstructured fluorescence spectra with intensity maxima at 331 and 325 nm, respectively. Upon addition of **FN** the fluorescence intensity decreases, but the shape of the bands remains unchanged. Formation of emitting secondary species is thus ruled out, and relative fluorescence quantum yields can be obtained directly by integrating the fluorescence spectra. Stern–Volmer plots were found to be linear within the range of quencher concentrations used ($c(\mathbf{FN}) \leq 0.1$ M). As the unquenched lifetimes τ_0^S of the excited anetholes **1A** are known (see Table 1), the rate constants k_q for quenching of **1tA** and **1cA** by **FN** can be determined from these plots; they are also listed in the table.

It has long been known¹⁸ that photodimerization of **tA** or **cA** leads to formation of ($\alpha,\alpha,\beta,\beta$)- and ($\alpha,\alpha,\alpha,\alpha$)-1,2-dianisyl-3,4-dimethylcyclobutane, respectively. These self-quenching reactions occur via intermediate excimers.^{18b} Owing to these processes, τ_0^S depends on the concentration of the substrate. However, in the experiments of the present work the anethole concentrations do not exceed 2×10^{-2} M. With the rate

(17) Eckert, G.; Goez, M. *J. Am. Chem. Soc.* **1994**, *116*, 11999–12009.

(18) (a) Nozaki, H.; Otani, I.; Noyori, R.; Kawanisi, M. *Tetrahedron* **1968**, *24*, 2183–2192. (b) Lewis, F. D.; Kojima, M. *J. Am. Chem. Soc.* **1988**, *110*, 8660–8864.

(11) (a) Lewis, F. D. *Acc. Chem. Res.* **1979**, *12*, 152–158. (b) Yang, N. C.; Yates, R. L.; Masnovi, J.; Shold, D. M.; Chiang, W. *Pure Appl. Chem.* **1979**, *51*, 173–180. (c) Caldwell, R. A.; Creed, D. *Acc. Chem. Res.* **1980**, *13*, 45–50. (d) Mattes, S. L.; Farid, S. *Acc. Chem. Res.* **1982**, *15*, 80–86.

(12) Wong, P. C.; Arnold, D. R. *Can. J. Chem.* **1979**, *57*, 1037–1049.

(13) Brown-Wensley, K. A.; Mattes, S. L.; Farid, S. *J. Am. Chem. Soc.* **1978**, *100*, 4162–4172.

(14) (a) *Chemically Induced Magnetic Polarization*; Lepley, A. R., Closs, G. L., Eds.; Wiley: New York, 1973. (b) Richard, C.; Granger, P. *Chemically Induced Dynamic Nuclear and Electron Polarizations—CIDNP and CIDEP*; Springer: Berlin, 1974. (c) Kaptein, R. *Adv. Free Rad. Chem.* **1975**, *5*, 319–381. (d) *Chemically Induced Magnetic Polarization*; Muus, L. T., Atkins, P. W., McLauchlan, K. A., Pedersen, J. B., Eds.; D. Reidel: Dordrecht, 1977. (e) Salikhov, K. M.; Molin, Yu. N.; Sagdeev, R. Z.; Buchachenko, A. L. *Spin Polarization and Magnetic Effects in Radical Reactions*; Elsevier: Amsterdam, 1984.

(15) (a) Roth, H. D. in ref 14d, pp 53–61. (b) Roth, H. D.; Manion, M. L. *J. Am. Chem. Soc.* **1975**, *97*, 6886–6888.

(16) Closs, G. L.; Miller, R. J. *J. Am. Chem. Soc.* **1979**, *101*, 1639–1641; **1981**, *103*, 3586–3588.

Table 2. Relative Energies of Intermediates in the Systems *cA*/FN, *tA*/FN, and *CNA*/*tA*^g

<i>E</i> [kJ mol ⁻¹]	<i>cA</i> /FN	<i>tA</i> /FN	<i>CNA</i> / <i>tA</i> /FN
<i>E</i> (¹ Q) ^a	510	510	510
<i>E</i> (¹ M) ^a	389	384	384
<i>E</i> (¹ S)			299 ^b
<i>E</i> (M ⁺ /S ⁻)			261
<i>E</i> (M ⁺ /Q ⁻)	267	260	260
<i>E</i> (³ Q) ^d	260	260	260
<i>E</i> (³ M)	355 ^e	250 ^f	250 ^f
<i>E</i> (³ S)			164 ^b

^a Determined from the turning points of the long-wave flanks in the fluorescence spectra. ^b Van der Donckt, E.; Barthels, M. R.; Delestine, A. J. *J. Photochem.* **1973**, *1*, 429–432. ^c From the redox potentials in acetonitrile vs SCE, positive values for the couples Φ (M⁺/M) and negative values for the couples Φ (M/M⁻): *cA*, +1.47 V;²¹ *tA*, +1.39 V;²¹ FN, -1.36 V (Arnold, D. R.; Wong, P. C. *J. Am. Chem. Soc.* **1979**, *101*, 1894–1895. Petrovitch, J. P.; Balzer, M. M.; Ort, M. R. *J. Electrochem. Soc.* **1969**, *116*, 743–749.); *CNA*, -1.37 V.²⁷ ^d Vertical triplet energy (Mirbach, M. J.; Mirbach, M. F.; Saus, A. *J. Photochem.* **1982**, *18*, 391–393). ^e AM1 calculations gave an energy difference between *cis*- and *trans*-anethole of 7 kJ mol⁻¹ in the ground state, and of 12 kJ mol⁻¹ in the triplet state. Our estimate of the vertical triplet energy given for ³*cA* is based on these results and on the experimental value for ³*tA*. ^f Vertical triplet energy (Caldwell, R. A.; Ghali, N. I.; Chien, C.-K.; DeMarco, D.; Smith, L. *J. Am. Chem. Soc.* **1978**, *100*, 2857–2863, ref 66). ^g M denotes the substrate (the respective anethole), Q the quencher FN, and S the auxiliary sensitizer (CNA) in the experiments with PET sensitization.

constants *k*_M for self-quenching given in Table 1 one arrives at a reduction of τ₀^S by about 5% in the worst case. Correction for this small effect was omitted.

Since ground-state complexes play no role in our reactions, the fact that *k*_q exceeds the rate of diffusion in acetonitrile tends to rule out desactivation of ¹A by formation of an exciplex ¹(A^{δ+}••FN^{δ-}), which is also consistent with the absence of exciplex emission from our systems; instead, it points to quenching by electron transfer occurring over distances larger than the collision diameter.¹⁹ Photoinduced electron transfer over distances up to 10.5 Å has also been observed in the reaction of *trans*-stilbene with FN in acetonitrile.²⁰ Further corroboration of electron transfer from ¹A to FN as the predominant quenching mechanism is provided by the CIDNP results presented below as well as by thermodynamic considerations.

Pertinent thermodynamical data of possible reaction intermediates are compiled in Table 2. Electron transfer quenching of ¹A is seen to be strongly exergonic (-Δ*G*⁰ > 120 kJ mol⁻¹) with both donors, so rapid quenching by this process is in accordance with expectations. The energetics show that back electron transfer of the resulting radical ion pairs A^{•+}FN⁻ is not necessarily restricted to the singlet state: Formation of triplet anethole ³A and FN in its ground state is thermodynamically feasible, as is formation of A and ³FN. The data for the reaction with the auxiliary sensitizer 9-cyanoanthracene have also been included in Table 2; these will be discussed in the section on photoinduced electron transfer sensitization.

Reaction Products. Apart from geometric isomerization of the substrate A as well as of the quencher, formation of cycloadducts takes place in the anethole–fumarodinitrile systems upon irradiation. Knowledge of the structure of these products is a prerequisite for the interpretation of the CIDNP experiments described below. While such structural identification can often be achieved on the basis of the CIDNP spectra

alone or by combining CIDNP detection with coherence transfer or decoupling techniques, this was not possible in our systems owing to severe overlap of signals. Hence we carried out the photoreaction on a preparative scale, isolated the products from the reaction mixture, and identified them separately. Apart from dimers of the substrate, different cross coupling products were found. Our main interest will be focussed on the latter in this study.

Besides traces of the already mentioned (α,α,β,β)-1,2-dianisyl-3,4-dimethylcyclobutane stemming from photodimerization via an exciplex^{18b} the only other dimer formed in detectable yield in the system *tA*/FN was characterized as the *all-trans* isomer (α,β,α,β)-1,2-dianisyl-3,4-dimethylcyclobutane, **D1**, which is known to result from cationic dimerization of *tA*.²¹ Its NMR parameters are given in the Experimental Section. As main products, however, four mixed adducts **P1–P4** (M⁺ = 226) were isolated and found to be stereoisomers of 1-anisyl-2-methyl-3,4-dicyanocyclobutane.

By their chemical shifts and multiplet patterns, the resonances of the methyl, the methoxy, and the aromatic protons could be identified trivially. Assignment of H² was straightforward by decoupling the methyl protons at the four-membered ring. By using NOE-difference experiments, we assigned the resonances of the other protons and determined the stereochemistry. For molecules of the size of our cycloadducts and in a solvent of low viscosity (acetonitrile) the extreme narrowing limit is realized at the NMR frequencies employed in this study. This leads to positive NOE enhancement factors for protons that are directly coupled by the dipolar interaction. Relaxation of the CH₃ protons predominantly occurs by dipolar relaxation among themselves, so only negligible NOE effects result at the methyl group when H¹ to H⁴ are saturated. In contrast, the dipolar coupling with the methyl protons provides an important relaxation mechanism for the cyclobutane protons in their spatial vicinity. Furthermore, with all four mixed adducts it turned out to be difficult or even impossible to saturate all the cyclobutane protons thoroughly enough and with adequate selectivity, since their signals are broad multiplets and partly possess very similar resonance frequencies. For these reasons, we saturated the methyl protons and the *ortho* protons of the anisyl group in each case, which was sufficient to fix the stereochemistry, and besides only a few of the cyclobutane protons for additional corroboration. The results are listed in Table 3 together with the structures of **P1–P4** that follow from these experiments.

The positive NOEs between H² and H⁴ in the cycloadduct **P1** as well as between H¹ and H³ in **P3** point to a nonplanar conformation of the cyclobutane skeleton, which moves these protons nearer to each other. For all four adducts, force-field computations predict a minimum energy for a cyclobutane ring folded by approximately 35° along the C²–C⁴-axis such that the anisyl substituent moves out radially. This is the same angle as in unsubstituted cyclobutane,²² which is slightly surprising because one would expect the voluminous anisyl group to cause higher Pitzer strain and consequently larger distortions. The transannular distance between pseudoaxial protons of the folded four-membered rings is calculated to be 2.65–2.75 Å. The value obtained for vicinal protons occupying *cis* positions is barely lower, 2.45 Å, so the *d*⁻⁶-dependence of dipolar relaxation should only lead to a difference of NOE enhancements in these two cases by a factor of about 2, in accordance

(19) Hub, W.; Schneider, S.; Dörr, F.; Oxman, J. D.; Lewis, F. D. *J. Am. Chem. Soc.* **1984**, *106*, 701–708.

(20) (a) Angel, S. A.; Peters, K. S. *J. Phys. Chem.* **1989**, *93*, 713–717. (b) Angel, S. A.; Peters, K. S. *J. Phys. Chem.* **1991**, *95*, 3606–3612. (c) Peters, K. S.; Lee, J. *J. Phys. Chem.* **1992**, *96*, 8941–8945.

(21) Lewis, F. D.; Kojima, M. *J. Am. Chem. Soc.* **1988**, *110*, 8664–8670.

(22) (a) Dows, D. A.; Rich, N. *J. Chem. Phys.* **1967**, *47*, 333–334. (b) Stone, J. M. R.; Mills, I. M. *Mol. Phys.* **1970**, *18*, 631–682. (c) Miller, F. A.; Capwell, R. *J. Spectrochim. Acta A* **1971**, *27*, 947–956.

Table 3. NOE Effects (at 250 MHz Except Where Noted) in the Four Mixed Adducts **P1–P4** and Resulting Stereochemistry^e

Compound	Saturation at	NOE Detection at					Structure
		H ¹	H ²	H ³	H ⁴	An ^b	
P1	An ^b	++	++		++	o	
	CH ₃	++	++	++			
	H ²	c	o	c	+	+	
P2	An ^b	++	++			o	
	CH ₃	++	++				
	H ²	c	o	c	c	++	
P3 ^c	An ^b	++	++ ^d			o	
	CH ₃	+	++ ^d	++ ^d	-		
	H ¹	o		++ ^d	++	++	
	H ⁴	++	++ ^d	o	+		
P4	An ^b	++	++		++	o	
	CH ₃	++	++				

^a Measured at 400 MHz. ^b Saturation or detection at the resonance frequency of the *ortho* protons of the anisyl substituent. ^c Determination not feasible owing to partial saturation caused by insufficient selectivity of the irradiation. ^d Superposition of the resonances of H² and H³ did not permit their separation in the NOE difference spectrum. However, with the stereochemistry of **P1**, **P2**, and **P4** known the question which of the remaining cyclobutane configurations **P3** possesses can already be decided on the basis of the NOE effects at H¹ and H⁴. The assignment of H² and H³ in the table is the only one consistent with the structure obtained. ^e Signal overlap did not permit exact determination of enhancement factors in all cases; hence only semiquantitative values (++, strong increase; +, small increase; -, small decrease; o, position of irradiation) are given. An denotes the anisyl moiety.

Table 4. Structures and NMR Parameters (in Acetonitrile-*d*₃ at Room Temperature) of the Four Cycloadducts **P1–P4**^d

δ [ppm]				
	P1	P2	P3	P4
$\delta(\text{CH}_3)$	1.219	1.279	1.218	1.231
$\delta(\text{H}^1)$	3.290	3.689	3.455	3.525
$\delta(\text{H}^2)$	2.743	3.266	3.234	2.807
$\delta(\text{H}^3)$	3.141	3.657	3.209	3.689
$\delta(\text{H}^4)$	3.420	3.863	3.899	3.486
$\delta(p\text{-OCH}_3)$	3.772	3.781	3.782	3.767
$\delta(\text{H}^{\text{ar}}, m)$	6.92 ^a	6.94 ^a	6.94 ^a	6.92 ^a
$\delta(\text{H}^{\text{ar}}, o)$	7.23 ^a	7.25 ^a	7.24 ^a	7.22 ^a
³ J _{2,Me}	6.55	6.79	6.00	6.79
³ J _{1,2}	10.06 (10.6)	9.369 (10.8)	10.8 ^b (10.9)	10.40 (10.7)
³ J _{2,3}	9.91 (10.2)	9.285 (8.2)	9.4 ^b (10.6)	8.31 (8.3)
³ J _{3,4}	9.78 (10.4)	4.286 (1.4)	8.38 (8.4)	8.21 (8.6)
³ J _{1,4}	10.33 (10.7)	9.181 (8.1)	7.39 (8.1)	10.54 (10.5)
⁴ J _{1,3}	c	-0.91	c	c
⁴ J _{2,4}	c	-0.88	c	c

^a Center of the multiplet; without simulation. ^b Exact determination impossible owing to the nearly identical chemical shifts of H² and H³. ^c Undetectable. ^d Coupling constants calculated by the Karplus–Conroy relation are given in parentheses. An denotes the anisyl moiety.

with the experimental observations. Finally, for the product **P3** a decrease of the signal of H⁴ is observed upon saturation of the methyl group. This can be explained by an indirect NOE (three-spin effect) via H¹ as well as H³.

From the spectra and with the NOE results, approximate NMR parameters of the cycloadducts were derived, which served as starting values for simulations of the *J*-coupled spin systems consisting of the cyclobutane protons and the methyl group. By iterative fitting of the simulated spectra to the experimental spectra, the chemical shifts and coupling constants displayed in Table 4 were obtained. These data are also consistent with the structures given. For each cyclobutane proton, the differences of the chemical shifts in the adducts **P1–**

P4 can be rationalized by the interplay of four factors. Two of these are due to the magnetic anisotropy of the cyano group. First, a pseudoaxial cyano group induces a small downfield shift of a transannular pseudoaxial proton (compare for instance H¹ in **P1** and **P4**). Second, for a vicinal proton in *cis* position to a cyano group a very slight upfield shift is observed, as, for example, H² in **P4** and in **P1** shows. Third, pseudoaxial protons have resonance frequencies that are a little lower than those of the corresponding pseudoequatorial protons (e.g., H³ in **P3** and **P4**), owing to the magnetic anisotropy of the C–C bonds of the cyclobutane skeleton and the methyl group. Fourth, the ring current of the anisyl group causes a noticeable diamagnetic shift of a vicinal *cis* proton (see H⁴ in **P2** and **P1**). All these trends in the chemical shifts are in line with expectations. Despite the smallness of the effects, their respective magnitudes are very similar for all four compounds, allowing one to describe the chemical shifts of H¹ to H⁴ with a set of increments. Lastly, in most cases the coupling constants extracted from the spectra agree very well with those computed by the Karplus–Conroy relation²³ from the molecular geometries predicted by the force-field calculations.

NMR spectra of the reaction mixture show the yields of the four cycloadducts **P1–P4** to be practically equal. Interestingly, with *cA* as the substrate instead of *tA* exactly the same mixed adducts are formed.²⁴ Hence, with both educts the configuration of the anethole-derived moiety in the cycloadducts is always *trans*. In contrast, with regard to the quencher-based moiety there is obviously a random distribution of all possible configurations.

Photoinduced Electron Transfer Sensitization. As explained above, our Stern–Volmer experiments pointed to formation of radical ion pairs, not exciplexes, from **1A** and **FN** as the predominant quenching mechanism. To test whether or not this pathway leads to the cycloadducts as well, we synthesized these products also by PET (photoinduced electron transfer) sensitization. In contrast to a “normal” sensitization experiment where the excited sensitizer **M*** is quenched by **Q**, with PET sensitization²⁵ an auxiliary sensitizer **S** is excited, **S*** is quenched by either **M** or **Q** to generate a primary radical ion pair, and the latter is then intercepted by the third reactant to give the same radical ion pair as upon direct sensitization but as a secondary species. For suitable energetic and kinetic parameters, neither electronically excited **M** nor electronically excited **Q** are touched upon before formation of the secondary radical ion pair. Mechanistic conclusions can then be drawn from the fact that in consequence this pair must be produced without the intervention of an exciplex **M^{δ±}...Q^{δ∓}**.¹⁷ If formation of the same products is observed in the direct and the PET-sensitized experiments, such an exciplex is obviously not a key intermediate for their generation.

For this purpose, 9-cyanoanthracene **CNA** was employed as auxiliary sensitizer for the reaction of *tA* with **FN**. It can be

(23) (a) Karplus, M. *J. Chem. Phys.* **1959**, *30*, 11–15. (b) Karplus, M. *J. Am. Chem. Soc.* **1963**, *85*, 2870–2871. (c) Sternhell, S. *Quart. Rev.* **1969**, *23*, 236–270.

(24) We should like to emphasize that the product distribution observed in these experiments does not unambiguously rule out that *tA* and *cA* react to different products: With our reactants cycloaddition is accompanied by geometric isomerization of the substrate to a large degree, so under conditions of preparative photolysis the system moves far towards the photostationary equilibrium between *tA* and *cA* regardless of whether the starting anethole is *cA* or *tA*. However, the same product distribution is also found in the CIDNP experiments described below, which are performed at very low conversion of the substrate.

(25) (a) Mattes, S. L.; Farid, S. In *Organic Photochemistry*; Padwa, A., Eds.; 1983; Vol. 6, pp 233–326. (b) Chanon, M.; Ebersson, L. In *Photoinduced Electron Transfer. Part A. Conceptual Basis*; Fox, M. A., Chanon, M., Eds.; Elsevier: New York, 1988; pp 409–597. (c) Mattay, J. *Synthesis* **1989**, 233–252.

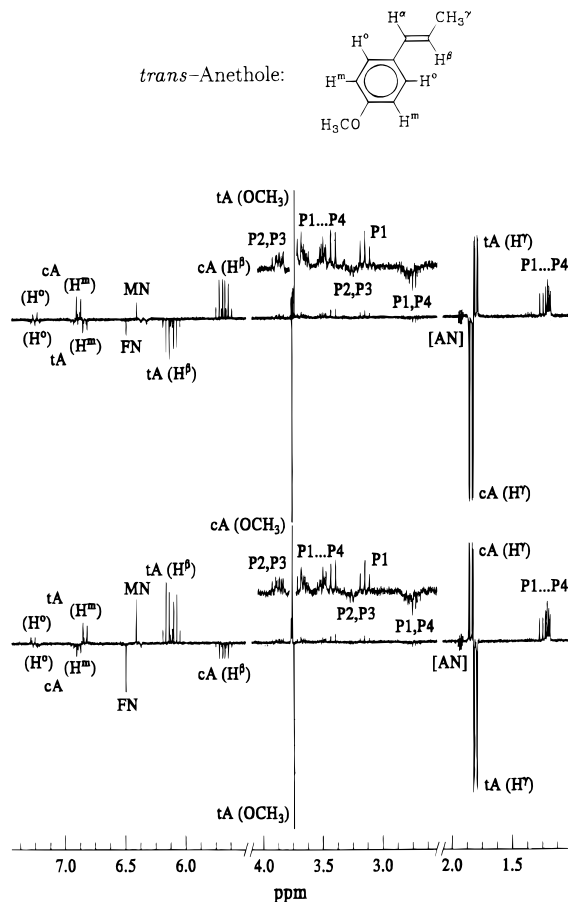


Figure 1. Background-free pseudo steady-state CIDNP spectra observed in the photoreactions of *trans*-anethole *tA* (bottom trace) and *cis*-anethole *cA* (top trace) with fumarodinitrile *FN* in acetonitrile-*d*₃ at room temperature. Experimental parameters, $c(tA) = 3 \times 10^{-3}$ M; $c(cA) = 2 \times 10^{-2}$ M; $c(FN) = 8 \times 10^{-3}$ M; $T = 274$ K. Amplitudes have been multiplied by a factor of 4 in the inset. The assignment of the resonances of *tA* refers to the structural formula given at the top; the same labels are used for the protons of *cA*. **P** denotes the cycloadducts **P1–P4**, the signals of which coincide partly. For this reason, only a few of the resonances of **P** are assigned in detail. These are denoted as in Table 3. The insufficiently suppressed signal marked [AN] is due to the solvent.

excited at $\lambda_{\text{exc}} \geq 385$ nm, where the other reactants as well as the ground-state complex between *tA* and *FN* do not absorb. The relevant thermodynamical parameters of the system *CNA/tA/FN* in acetonitrile have been given in Table 2. With these data, it is seen that singlet–singlet energy transfer from ¹CNA to *tA* or to *FN* can be ruled out as it would be much too endergonic. Quenching of ¹CNA by electron transfer from *tA* is exergonic by about 40 kJ mol⁻¹, so it is assumed to proceed diffusion controlled. With τ_0^S of ¹CNA being 17 ns,²⁷ quantum yields for formation of the primary radical ion pair *tA*^{•+}*CNA*^{•-} should be at least 80% at the concentration of *tA* used in our experiment (0.025 M). Although thermodynamics indicate back electron transfer of the radical ion pairs *tA*^{•+}*CNA*^{•-} to give ³A to be feasible, we found that in the absence of *FN* these pairs decay almost exclusively by back electron transfer to ³CNA, making the system *CNA/tA* very photostable. Presumably, this behavior is due to the very low triplet energy of the auxiliary sensitizer in comparison to the triplet energy of the substrate. Interception of *tA*^{•+}*CNA*^{•-} by *FN* is not as favorable thermo-

dynamically as is formation of this radical pair; owing to the almost identical reduction potentials of *CNA* and *FN* the driving force of this process is nearly zero, and the rate constant is estimated to be lower than the diffusion-controlled limit by about one order of magnitude.²⁸ Thus, this reaction should proceed on a time scale of some 10 ns under the experimental conditions ($c(FN) = 0.1$ M); still, as this is comparable to the life of the pair^{14c} a substantial amount of *tA*^{•+}*FN*^{•-} is expected to result.

The same cycloadducts were found in this experiment with PET sensitization as in the direct reaction of ¹*tA* with *FN*, and their yields were good enough to utilize this method for preparative generation of **P1–P4**. These observations clearly demonstrate that the route via the radical ion pairs *tA*^{•+}*FN*^{•-} is at least a major, if not the predominant, pathway to the cycloadducts. On the other hand, as our quenching studies furnished evidence that electron transfer quenching of ¹A prevails over quenching by exciplex formation, exciplexes preceding the radical ion pairs may also be disregarded. In combination, these findings show that ¹(A^{δ+}...*FN*^{δ-}) does not play an important mechanistic role in the cycloadditions of *A* and *FN*.

CIDNP Spectra. As shown in Figure 1, strong CIDNP signals arise during the photoreactions of *tA* or *cA* with *FN*. Nuclear spin polarizations are observed for the starting anethole and its respective isomerization product, for the quencher *FN* and its *cis* isomer maleodinitrile *MN*, and for the four cycloadducts **P1–P4**.

Qualitative mechanistic information can be extracted from these spectra with Kaptein's rule for CIDNP net effects,³⁰

$$\Gamma_i = \text{sgn}a_i \times \text{sgn}\Delta g \times \mu \times \epsilon \quad (1)$$

Equation 1 connects the polarization phase ($\Gamma_i = +1$, absorption, $\Gamma_i = -1$, emission) of proton *i* in a particular reaction product with magnetic parameters of the intermediate radical pairs with magnetic parameters of the intermediate radical pairs ($\text{sgn}a_i$, sign of the hyperfine coupling constant of the proton considered; $\text{sgn}\Delta g$, sign of the difference of the *g* values of the two radicals constituting the pair, where the radical counted first contains the proton in question) and with the entry and exit channels of the pairs ($\mu = +1$, pair formation from triplet precursors; $\mu = -1$, from singlet precursors; $\epsilon = +1$, product resulting from singlet radical pairs; $\epsilon = -1$, from triplet pairs).³¹ In addition,

(28) As ΔG^0 for interception of *tA*^{•+}*CNA*^{•-} by *FN* is almost zero, the rate constant for this process is approximately given by the geometric mean of the rate constants k_{ex} for the self exchange in the systems *FN/FN*^{•-} and *CNA/CNA*^{•-} (Kavarnos, G. J.; Turro, N. J. *Chem. Rev.* **1986**, *86*, 401–449). CIDNP measurements show the former rate constant in acetonitrile to be as high as 1×10^9 M⁻¹ s⁻¹ even at 235 K (Eckert, G. Ph.D. Thesis, Braunschweig, 1995); at room temperature the structurally very similar tetracyanoethylene has²⁹ $k_{\text{ex}} = 2.5 \times 10^9$ M⁻¹ s⁻¹. An estimate for the self-exchange rate constant of the couple *CNA/CNA*^{•-} is provided by the value for 9,10-diaminoanthracene, $k_{\text{ex}} = 2.5 \times 10^9$ M⁻¹ s⁻¹ in acetonitrile at 293 K (Grampp, G.; Jaenicke, W. *Ber. Bunsenges. Phys. Chem.* **1984**, *88*, 325–334), since k_{ex} is comparable for systems of related structure, and anions seem to possess somewhat higher k_{ex} than cations (see the examples in ref 29). A rate constant of at least 2×10^9 M⁻¹ s⁻¹ thus seems reasonable for the interception process. However, even a much smaller value would not invalidate our conclusions owing to the lack of other desactivation pathways of *tA*^{•+}*CNA*^{•-} besides interception by *FN* and back electron transfer to give ³CNA.

(29) Grampp, G.; Harrer, W.; Jaenicke, W. *J. Chem. Soc., Faraday Trans. 1* **1987**, *83*, 161–166.

(30) Kaptein, R. *J. Chem. Soc., Chem. Commun.* **1971**, 732–733.

(31) According to the usual definition of ϵ , this parameter is taken to denote the mode of product formation ($\epsilon = +1$, cage reaction; $\epsilon = -1$, reaction of escaping radicals). This interpretation is appealing to chemists because it is directly linked to mechanistic concepts; very often it is also permissible, since for the majority of radical pairs cage recombination can take place in the singlet state only. In reactions involving radical ion pairs, however, geminate processes of pairs of either multiplicity are frequently possible, so the assignment of ϵ (Roth, H. D.; Manion-Schilling, M. L. *J. Am. Chem. Soc.* **1980**, *102*, 4303–4310) adopted here must be used.

(26) For photoinduced electron transfer sensitization in a similar reaction system see ref 13.

(27) Lewis, F. D.; Bedell, A. M.; Dykstra, R. E.; Elbert, J. E.; Gould, I. R.; Farid, S. *J. Am. Chem. Soc.* **1990**, *112*, 8055–8064.

for a given product the polarization intensity of a group of equivalent protons i divided by their number, P_i , reflects the magnitude of a_i ; if Δg is large, there is even approximate proportionality between P_i and a_i .^{14c} Hence, the polarization patterns, i.e., the relative CIDNP intensities of the different protons in a product, yield information almost equivalent to an EPR spectrum of the intermediates with the additional benefit that each hyperfine coupling constant can be related directly to a specific proton.^{15,32}

With regard to the starting anethole, one obtains from Figure 1 that $P_{H\beta} \approx -P_{H\gamma} \gg -P_{OCH_3} > P_{H^{3,5}} > P_{H^{2,6}} \approx -P_{H^a}$ (for the assignment see the figure). These intensity patterns are in good agreement with the calculated¹⁷ spin density distributions in the radical cations $tA^{+\bullet}$ or $cA^{+\bullet}$ of the anetholes. Besides, quantitatively the same patterns are found in the reactions of tA and cA with quinones, for which it was shown that CIDNP originates from radical ion pairs comprising $tA^{+\bullet}$ and $cA^{+\bullet}$, respectively.¹⁷ Together with the results of our quenching studies, this furnishes proof that the observed polarizations are generated in radical ion pairs $A^{+\bullet}FN^{\bullet-}$, where $A^{+\bullet}$ is the radical cation of the respective anethole.

As can be seen in both spectra of Figure 1, the polarizations of the isomerized anethole are mirror images of the polarizations of the starting anethole. This is clear evidence that these two species result from opposite exit channels of the same intermediate pairs. The polarization patterns of all four cycloadducts are equal to those of the isomerized substrate; in addition, the phases of the corresponding protons are identical in these two classes of products (compare, for instance, the methyl groups in the isomerized anethole and in **P1–P4**, both being the most strongly polarized signals of these compounds and exhibiting enhanced absorption). Cycloadducts and isomerized substrate are thus formed via the same exit channel of the radical ion pairs.

The fact that the cycloadduct signals are absolutely identical in the two spectra of Figure 1 convincingly demonstrates that the reaction via radical ion pairs leads to the same adducts regardless of the configuration of the starting anethole. From an analysis of the superposition signal due to the methyl groups in these four different products, it is further seen that the yields of **P1–P4** are practically equal. This simple evaluation is permissible because protons are being considered that were identical in the intermediates, and because the CIDNP spectra presented are free from the effects of nuclear-spin relaxation both in the products and the intermediates. The former is a consequence of the experimental technique (pseudo steady-state photo-CIDNP measurements).³³ The latter can be concluded from the fact that the integral over all CIDNP signals of protons having a common source (e.g., the methyl protons in the starting and the isomerized anethole, and those in **P1–P4**) vanishes, which was found to hold for all the CIDNP spectra of this work. Compared to conventional studies of the product distribution, these CIDNP determinations of relative yields possess the advantage that they are performed at fairly low conversion of the starting anethole to its geometric isomer (less than 5% in our measurements). This is feasible, since the signal enhancement by the CIDNP effect allows one to detect also products formed in low amounts, hence at low turnover, while maintaining the analytic potential of high-resolution NMR. On the other hand, the very strong nuclear-spin polarizations and the results of our fluorescence quenching and PET-sensitization studies, which bear out formation of radical ion pairs as key intermediates, exclude the possibility that the CIDNP signals are merely

due to a side-reaction, whereas the products predominantly stem from nonradical pathways.

By inspection of the two spectra of Figure 1, one can immediately rule out that the observed isomerization of the anetholes takes place before, or concomitantly with, CIDNP generation, because in that case the same CIDNP signals would be obtained as with a mixture of tA and cA , that is, the same polarization phases would result for the starting as well as the isomerized substrate. The unimportance of geometric isomerization of 1A in our measurements also follows from the photophysical data and the results of our quenching studies: With the values given in Table 1, one calculates a quantum yield of geometric isomerization of 4% for 1tA and of 2% for 1cA under the experimental conditions of Figure 1, taking into account the temperature dependence of k_q with the Smoluchowski equation and the known³⁴ viscosities of acetonitrile, while quantum yields for radical ion pair formation lie above 65% in these two cases. Likewise, the fact that no isomerization of the radical ions occurs is not surprising as the configurational stability of anethole radical cations has been verified both theoretically¹⁷ and experimentally.^{9,17,21}

It is well known that olefin isomerization accompanying cycloaddition can also take place by bond rotation in a triplet biradical³⁵ or via the olefin triplet.^{9,15,36} In a previous study of quinone-sensitized anethole photoreactions,¹⁷ where 3A cannot be formed for energetic reasons, we found the biradical pathway to lead to efficient one-way *cis–trans* isomerization of the starting olefin, paralleling the distribution of configurations of the anethole moiety in the cycloadducts. In the present instance, the configuration of the anethole part is *trans* in all four adducts, so there is again one-way *cis–trans* isomerization of the anethole fragment as far as cycloaddition is concerned, but isomerization of the substrate proceeds in both directions, as is evident from Figure 1, bottom trace. Hence, isomerization of the substrate must be ascribed chiefly to the triplet state of the anethole, the formation of which is thermodynamically feasible in our systems (compare Table 2), while a participation of the biradical pathway is not excluded by these qualitative arguments. In both cases, however, the key intermediate between the radical ion pair and the isomerized substrate is a triplet species, making the parameter ϵ of Kaptein's rule negative. With the precursor multiplicity being singlet, it follows from the absorptive polarizations of the methyl protons ($a > 0$) in the isomerized anetholes that $tA^{+\bullet}$ and $cA^{+\bullet}$ possess larger g values than does $FN^{\bullet-}$.

Geometric isomerization of the quencher **FN** manifests itself by the CIDNP signals of the vinyl protons of **MN** observed in both photoredox systems. The absorptive polarizations of these protons ($a < 0$) show that this process again occurs via the triplet exit channel of the radical ion pairs. This cannot be explained by free radical ions escaping from triplet pairs, because $FN^{\bullet-}$ is configurationally stable.³⁷ Furthermore, from the fact that isomerization of the anetholes via the biradical route is obviously not predominant it also follows that this mechanism is of secondary importance in the case of **FN**, since the same intermediates would be involved in the isomerizations of both the substrate and the quencher by that pathway. Hence, isomerization of the quencher must also take place mainly by

(34) Grampp, G.; Jaenicke, W. *Ber. Bunsenges. Phys. Chem.* **1984**, *88*, 335–340.

(35) Caldwell, R. A.; Sovocool, G. W.; Gajewski, R. P. *J. Am. Chem. Soc.* **1973**, *95*, 2549–2557.

(36) Arnold, D. R. *Adv. Photochem.* **1968**, *6*, 301–423.

(37) In time-resolved CIDNP studies of the self-exchange between $FN^{\bullet-}$ and **FN** we did not find any evidence for geometric isomerization of the free radicals $FN^{\bullet-}$ on a time scale of 10 μ s (Eckert, G. Ph.D. Thesis, Braunschweig, 1995).

(32) Roth, H. D. Z. *Phys. Chem. Neue Folge* **1993**, *180*, 135–158.

(33) Goetz, M. *Chem. Phys. Lett.* **1992**, *188*, 451–456.

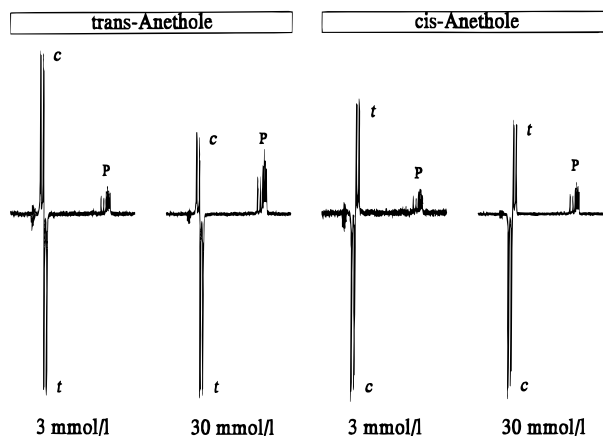


Figure 2. Dependence of the polarization intensities of the respective isomerized anethole and the cycloadducts on the concentration (given at the traces) of the quencher fumarodinitrile. The spectra (range 1.0–2.1 ppm) displaying the resonances of the methyl groups in educts and products have been normalized to equal height of the emission signal of the starting anethole.

the triplet route and population of ${}^3\text{FN}$, which is nearly isoenergetic with ${}^3\text{A}$ (Table 2), must provide an additional decay pathway of the pairs ${}^3\text{A}^+\text{FN}^{\bullet-}$.

Finally, the protons of both the anethole- and the fumarodinitrile-derived moieties in the cycloadducts **P1–P4** are polarized, as is seen from the signals of the cyclobutane protons in the spectral range between 2.5 and 4.0 ppm. The ratio of their CIDNP intensities agrees well with the ratio of the hyperfine coupling constants of the respective protons in the anethole cations and the quencher anions. This confirms that the intermediate pairs comprise both $\text{A}^{\bullet+}$ and $\text{FN}^{\bullet-}$.

In a recently published investigation of the Paterno–Büchi reaction of anetholes with quinones in polar media,¹⁷ we found that the cycloadducts were formed by geminate combination of correlated radical ion pairs in triplet states to give triplet biradicals, whereas back electron transfer of the singlet pairs regained the educts; a significant participation of free radical ions could be excluded. The results of the CIDNP experiments of this section suggest that the same mechanism is realized in the [2 + 2] photocycloaddition of the present work, with the modification that in the anethole/fumarodinitrile systems back electron transfer is also possible for triplet pairs and leads to bidirectional geometric isomerization of donor and acceptor olefin. The low yield of dimers such as **D1**, which is known²¹ to result from a cationic route, and which can thus be formed much more efficiently by attack of (long-lived) escaping radical cations $t\text{A}^{\bullet+}$ to surplus substrate than by combination of $t\text{A}^{\bullet+}$ and $t\text{A}$ during diffusive excursions of the radical ions (i.e., during the much shorter correlated life of the pairs), indicates that free radicals do not play a significant role also in our systems.³⁸ This is further corroborated by the absence of relaxation loss, as well as by the time-resolved CIDNP measurements and scavenging experiments described below.

Concentration Dependence of the CIDNP Intensities.

Figure 2 shows part of the CIDNP spectra of our systems (resonances of the methyl protons in the starting and isomerized anethole, and in the cycloadducts **P1–P4**) at two different

(38) As the spectra of Figure 1 show, no CIDNP signals can be detected for the dimers. On the one hand, we attribute this to the low yields of these products, and on the other hand, the primary species resulting from combination of radical ion and substrate is still a radical ion. The nuclear spin polarization generated in the radical ion pairs will therefore be largely destroyed by nuclear spin relaxation during the life of the free paramagnetic species. Absence of CIDNP in dimer formation has also been reported for other systems.^{15a}

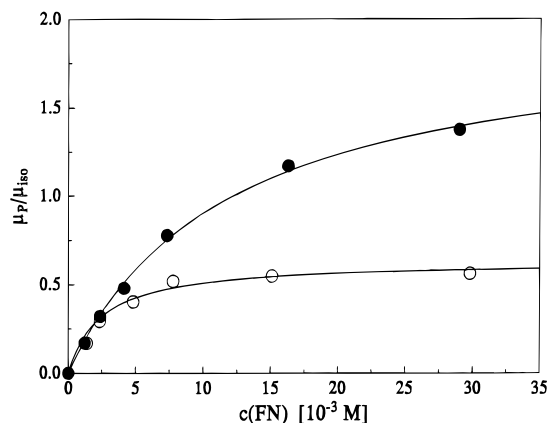


Figure 3. Ratios μ_p/μ_{iso} of the polarizations of the cycloadducts and the isomerized substrate as a function of the fumarodinitrile concentration.³⁹ Filled and open circles, starting anethole $t\text{A}$ and $c\text{A}$, respectively. Experimental parameters: $c(t\text{A}) = 3.3 \times 10^{-3} \text{ M}$, $c(c\text{A}) = 1.98 \times 10^{-2} \text{ M}$, $T = 273 \text{ K}$.

concentrations of the quencher **FN**. From these spectra it is obvious that in the reaction of $t\text{A}$ with **FN** an increase of the quencher concentration leads to a significant increase of these polarizations in the photoadducts, while the signal that is due to the isomerized substrate decreases by the same amount. Although less pronounced, this effect is also observed with $c\text{A}$ as starting material.

Quantitative investigation of this concentration dependence is complicated by partial isomerization of the anethole during the measurements, which cannot be avoided. Despite the fact that typically the degree of isomerization does not amount to more than 5%, this leads to significant changes of relative CIDNP signal strengths in the system $c\text{A}/\text{FN}$ because at the excitation wavelength the extinction coefficient of the *trans* isomer accumulated during the experiment is about 10 times higher than that of $c\text{A}$; quantitative analysis would thus be impossible without appropriate correction. However, at low consumption of the substrate, the composition of the sample changes practically linearly with the number n of laser flashes already absorbed, and so do the CIDNP intensities. For each sample we therefore recorded several CIDNP spectra in succession, hence at different values of n , and then extrapolated the polarizations to $n = 0$. All CIDNP intensities evaluated in the following were corrected in this way, but with $t\text{A}$ as the substrate this correction was invariably very small. In no case did we observe significant deviations from linearity.

In Figure 3, the ratios μ_p/μ_{iso} of the polarizations of the cycloadducts and the isomerized substrate have been plotted as functions of the quencher concentration for both photoredox systems. For given net polarization of a proton in a radical pair, which only depends on the magnetic parameters and the correlated life of the pair, and in the absence of nuclear spin relaxation, the polarizations of the corresponding protons in the products are directly proportional to the product yields. With a simple kinetic scheme comprising two competing decay reactions of a single radical pair, one leading to cycloaddition, the other to isomerization, a constant value of μ_p/μ_{iso} would thus be expected. This is indeed found at high quencher concentrations, but the decrease of this ratio with decreasing concentration of **FN** shows that the mechanism must be more complicated.

(39) The curves through the data points in Figure 3 as well as Figure 4 were drawn as best fits according to a theoretical model for the concentration dependence of the CIDNP intensities, which is outside the scope of the present work and will be published separately.⁶⁵

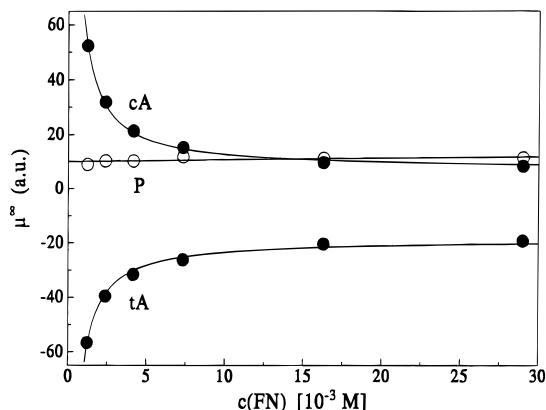


Figure 4. Polarizations μ^∞ referred to unit quantum yield of radical ion pair formation in the system tA/FN .³⁹ Experimental parameters as in Figure 3.

Besides, and most strikingly, small but noticeable polarizations of the starting and the isomerized anethole were also observed in the absence of FN . The polarization patterns and CIDNP phases of these two species were the same as in Figure 1. These findings indicate the presence of a parallel isomerization pathway via another radical ion pair besides $A^{+\bullet}FN^{\bullet-}$. As suggested by the CIDNP data, this second pair also comprises the anethole radical cation but a radical anion other than $FN^{\bullet-}$; the latter, $X^{\bullet-}$, possesses a lower g value than does $A^{+\bullet}$.

Further information was obtained by evaluating the absolute polarizations rather than their ratio. In this instance, however, an additional correction must be performed because CIDNP signal strengths are directly proportional to the concentration of the radical pairs, which in turn is a function of the quencher concentration. Measured signals were therefore multiplied by $1 + [k_q\tau_0^S c(FN)]^{-1}$ to refer them to unit quantum yield Φ_{RP} for radical ion pair formation. Changes in the amount of light absorbed by different samples were minimized by carrying out all measurements of a series in immediate succession, in identical NMR tubes, without changing the optical setup, and at the same laser energy. The polarizations μ^∞ obtained in this way have been plotted in Figure 4 as a function of the quencher concentration. The low fluctuations of the data establish the feasibility of this procedure.

It is evident from the figure that the efficiency of cycloadduct formation from the radical ion pairs $A^{+\bullet}FN^{\bullet-}$ is independent of the quencher concentration. The divergence of the polarizations $\mu^\infty(cA)$ and $\mu^\infty(tA)$ for vanishing quencher concentration is due to the correction of these CIDNP signals by the factor $1 + [k_q\tau_0^S c(FN)]^{-1}$, which is solely applicable for that fraction of them stemming from the pairs $A^{+\bullet}FN^{\bullet-}$. If that correction is omitted, the absolute values of these polarizations start at a finite intercept; they increase with increasing quencher concentration, though initially slower than $k_q\tau_0^S c(FN)/[1 + k_q\tau_0^S c(FN)]$, i.e.

than the quantum yield of formation of $A^{+\bullet}FN^{\bullet-}$; finally, they approach a constant level. On the one hand, the fact that the limiting polarizations are higher than the polarizations in the absence of quencher confirms that isomerization does not only occur in the as yet unidentified radical pair but also in $A^{+\bullet}FN^{\bullet-}$. On the other hand, the observed concentration dependence of the absolute polarizations of tA and cA points to a competitive formation of both types of radical pairs.

Polarographic determination gave a value of -1.98 V vs SCE for the potential of the redox couple $tA/tA^{\bullet-}$ in acetonitrile, so

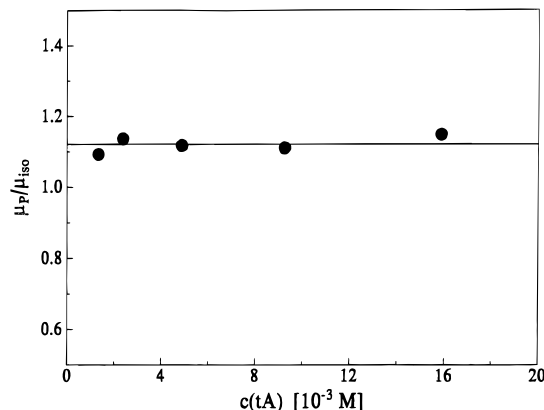


Figure 5. Dependence of the polarization ratio μ_p/μ_{iso} on the substrate concentration in the system tA/FN . Experimental parameters: $c(FN) = 1.5 \times 10^{-2}$ M, $T = 273$ K.

the free enthalpy of the radical ion pair $tA^{+\bullet}tA^{\bullet-}$ lies some 60 kJ mol⁻¹ below that of 1tA (compare Tables 1 and 2). Photoinduced disproportionation of the substrate is thus thermodynamically feasible; also, as mentioned above, self-quenching of anetholes is a known reaction.^{18b} To test whether the isomerization of the substrate occurring without the intervention of FN relies on this process, we kept the quencher concentration at a moderate value and varied the anethole concentration. As Figure 5 shows, the polarization ratio μ_p/μ_{iso} is independent of $c(tA)$. This definitely rules out the pair $tA^{+\bullet}tA^{\bullet-}$ as the intermediate leading to the polarizations found in the absence of FN . This is also consistent with expectations, because even if such pairs were formed it seems very doubtful whether they could lead to noticeable polarizations in the starting and the isomerized anethole.⁴⁰

The most trivial explanation of the polarizations found in the samples without FN would be an impurity that acted either as sensitizer or as quencher of the excited anetholes. We could not detect the presence of an additional light-absorbing substance in the UV/vis spectra of the substrates nor in the spectrum of the acetonitrile employed; besides, this would lead to a dependence of the polarization ratios on the substrate concentration, which is not found (Figure 5). Owing to the short lifetimes of excited species, quenching by an impurity would demand that this were present in quite high concentration; hence it could only have been contained in the solvent used for the CIDNP experiments, not in the starting anethole, the purity of which was at least 99.5% and which was itself employed in millimolar concentrations only. Since we could not observe it in the NMR spectra, it would have to be a perdeuterated compound. We could not find any evidence for the presence of such a species in our solvent by optical spectroscopy; furthermore, we observed identical CIDNP spectra of our systems with solvents purchased from different manufacturers. On these grounds, we are inclined to rule out the impurity hypothesis.

The observed substrate isomerization without participation of FN can thus only be explained by a reaction of the excited anethole with the solvent to give radical ion pairs.

(40) Calculations show the spin density distributions of $tA^{+\bullet}$ and $tA^{\bullet-}$ to be similar. For the aromatic protons this follows also from the pairing theorem. Corresponding protons in the radical cation and the anion of the pairs $tA^{+\bullet}tA^{\bullet-}$ would therefore bear opposite polarizations of comparable magnitude. These would largely cancel in back electron transfer of singlet pairs, because $tA^{+\bullet}$ and $tA^{\bullet-}$ react to the same species, and also in back electron transfer of triplet pairs, because in this process there is no preference for formation of 3tA or tA from the cation or the anion. This argument can be extended to isomerization via bond rotation in a triplet biradical followed by biradical cleavage.

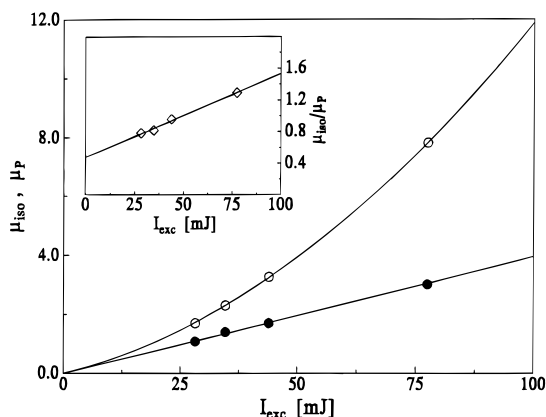


Figure 6. Polarizations of the cycloadducts μ_P (filled circles) and of the isomerized substrate μ_{iso} (open circles) in the system *tA*/FN as functions of the light intensity I_{exc} . For clarity, μ_{iso} has been multiplied by a factor of 2. Experimental parameters: $c(tA) = 3 \times 10^{-3}$ M, $c(FN) = 8 \times 10^{-3}$ M, $T = 251$ K. The fit curves to μ_P and μ_{iso} are given by eqs 2 and 3. The inset shows a plot of the ratio μ_{iso}/μ_P as a function of I_{exc} .

Influence of the Laser Intensity. Plots of the CIDNP signal strengths for the cycloadducts and the isomerized substrate as functions of the intensity I_{exc} of the excitation light are given in Figure 6. As adduct formation was shown to occur via the radical ion pairs $A^{+\bullet}FN^{\bullet-}$, which are produced by electron transfer quenching of 1A , it is natural to assume that the polarizations μ_P are proportional to I_{exc}

$$\mu_P = \chi_{1,P} \cdot I_{exc} \quad (2)$$

where the constant $\chi_{1,P}$ comprises among other things the CIDNP enhancement factor for this radical pair. Equation 2 holds, as can be seen in the figure.

Surprisingly, however, at low quencher concentrations μ_{iso} grows faster than linearly with increasing I_{exc} . These data can be fitted with a function composed of a term quadratic in I_{exc} and a term linear in I_{exc} (compare Figure 6). Since the CIDNP experiments at variable quencher concentration furnished evidence that 1A is deactivated by two competitive processes leading to two radical pairs and that both these pairs provide pathways for isomerization of the substrate, the polarizations μ_{iso} must indeed comprise a term linear in I_{exc} due to the pair $A^{+\bullet}FN^{\bullet-}$; obviously, the term caused by the other pair depends on the square of the light intensity

$$\mu_{iso} = \chi_{1,iso} \cdot I_{exc} + \chi_{2,iso} \cdot I_{exc}^2 \quad (3)$$

The ratio μ_{iso}/μ_P is thus proportional to I_{exc} and possesses a nonzero limiting value of $\chi_{1,iso}/\chi_{1,P}$ for vanishing I_{exc} , as the inset of Figure 6 shows. From the former observation, it immediately follows that the additional radical pair is produced by a two-quantum process, whereas the latter observation once more confirms that isomerization takes place via both pairs.

At large quencher concentrations the linear dependence of the product polarizations μ_P on the light intensity remains unchanged whereas the curve for μ_{iso} is flattened out as to become practically linear as well. This clearly reflects the fact that formation of the two radical pairs occurs by competitive reactions, a high concentration of FN favoring quenching, i.e., the monophotonic pathway and suppressing the biphotonic process.

Temperature Dependence. Figure 7 displays plots of the temperature dependence of the polarization ratios μ_P/μ_{iso} in the

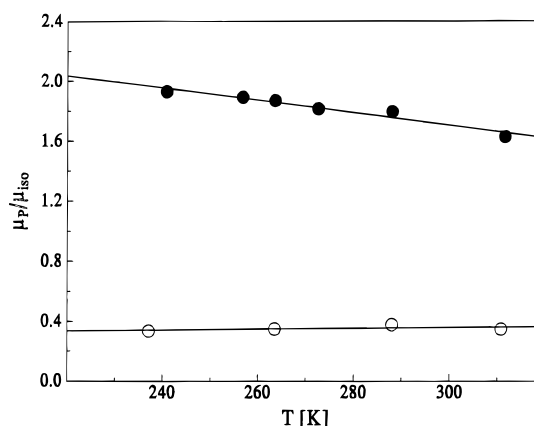


Figure 7. Influence of temperature on the ratio μ_P/μ_{iso} of cycloadduct polarizations and polarizations of the isomerized anethole in the systems *tA*/FN (filled circles) and *cA*/FN (open circles). Experimental parameters: $c(tA) = 4.2 \times 10^{-3}$ M, $c(FN) = 1.5 \times 10^{-1}$ M, and $c(cA) = 8 \times 10^{-3}$ M, $c(FN) = 2.4 \times 10^{-2}$ M, respectively.

systems *tA*/FN and *cA*/FN at large quencher concentration, i.e., in the plateau regime of Figure 3. It is seen that quite different behavior is found in these two instances: in the former case, an increase of the temperature leads to a noticeable decrease of the polarization ratio, while in the latter case the influence of the experimental temperature is negligible.

CIDNP enhancement factors are functions of temperature through their dependence on the diffusion coefficient.^{14d,e} However, this is eliminated by considering ratios of polarizations. The experimental conditions in these measurements were such that the biphotonic process was suppressed so strongly as to be undetectable. Hence, all polarizations exclusively stem from the radical ion pairs $A^{+\bullet}FN^{\bullet-}$, and the observed effects must be attributed to processes occurring at later stages of the reaction than these pairs.

Time-Resolved CIDNP Measurements and Scavenging Experiments. As has already been established above, olefin isomerization involving the pairs $A^{+\bullet}FN^{\bullet-}$ chiefly occurs by back electron transfer of triplet pairs in our systems, yielding one of the triplet species 3A or 3FN . However, with regard to cycloaddition, which also takes place via the triplet exit channel of $A^{+\bullet}FN^{\bullet-}$, a mechanistic question is left open: **P1–P4** may result from geminate combination of the triplet pairs yielding triplet species (e.g., triplet biradicals), which then decay to the species detected, or they may be formed by escape from the cage to give free radicals, which ultimately react further to the cycloadducts. In the photocycloadditions of anetholes with quinones we found the first possibility to be realized;¹⁷ on the other hand, formation of free radicals is the most common decay pathway of triplet radical pairs. A differentiation between these alternatives is possible because the former occurs on a nanosecond time scale, whereas the second is much slower. Hence, the two can be distinguished either by time-resolved CIDNP measurements (“flash CIDNP”)¹⁶ or by scavenging experiments.

In samples with very low concentrations of *tA* ($c(tA) < 1 \times 10^{-3}$ M), we observed a time dependence of the signal due to the starting anethole. The intensity of this emissive signal was largest immediately after the flash and then decreased by some 30% within a few microseconds. This can be explained by cancellation of the geminate polarizations in *tA*, which appear instantaneously on the time scale of these measurements, by the opposite polarizations in escaping $tA^{+\bullet}$ that are gradually transferred to *tA* by degenerate electron exchange with surplus substrate, a phenomenon that is well known in CIDNP

investigations of electron transfer reactions.⁴¹ In contrast, we could not detect any change of the signals due to the isomerized olefin and the cycloadducts. Owing to the low optical density of these samples and the lower sensitivity of flash-CIDNP measurements in comparison to pseudo steady-state CIDNP experiments, all signals were very weak. While experimental error was thus too large to permit quantitative evaluation, these results may be taken to indicate that some amount of free radicals is indeed formed. However, their polarizations evidently do not appear in the cycloadducts nor in the isomerized anethole but are predominantly transferred back to the starting anethole by degenerate electron exchange; from the above-mentioned absence of relaxation losses in the pseudo steady-state experiments it is clear that a decay of these polarizations by nuclear-spin relaxation in the free radicals or in subsequent paramagnetic species is negligible.

Because of its low oxidation potential (+1.12 V in acetonitrile vs SCE),⁴² 1,2,4-trimethoxybenzene **TMB** has repeatedly been employed to scavenge radical cations.^{9,43} As the reduction of free $t\mathbf{A}^+$ by **TMB** is exergonic by 26 kJ mol⁻¹, this reaction should be diffusion controlled. In the system $t\mathbf{A}/\mathbf{FN}$ ($c(t\mathbf{A}) = 2 \times 10^{-2}$ M, $c(\mathbf{FN}) = 8 \times 10^{-3}$ M, $T = 279$ K), absolute polarizations of the cycloadducts were somewhat reduced upon addition of **TMB**, by some 4, 14, 20, and 22% at scavenger concentrations of 2×10^{-3} , 4×10^{-3} , 6×10^{-3} , and 9×10^{-3} M, respectively. This decrease can be ascribed partly to absorption of the excitation light by the sensitizer, the extinction coefficient of **TMB** at 308 nm being about 10% of that of $t\mathbf{A}$, partly to quenching of $t\mathbf{A}$ by **TMB**, which should be exergonic by more than 80 kJ mol⁻¹, and partly to interception of the correlated radical pairs $t\mathbf{A}^+\mathbf{FN}^{\bullet-}$ by the scavenger. However, even at the lowest concentration of **TMB** employed the life of free anethole cations is calculated to be reduced to less than 30 ns; this should lead to almost complete quenching of all escape polarizations, yet only a very small effect on the polarizations is found in that case. An involvement of free radicals in cycloadduct formation is thus ruled out for the pathway giving rise to CIDNP.

It is well known that various nucleophiles readily add to the double bond of the radical cations of aryl olefins.^{9,25a,44} Despite the moderate reactivity of β -substituted derivatives of styrene toward methanol,⁴⁴ reactions involving free anethole cations should be detectably suppressed if high concentrations of this alcohol are employed. However, even in neat CD₃OD the CIDNP signals of the olefins and of **P1–P4** persisted, and we did not observe any polarizations indicating formation of scavenging products. This further corroborates a pathway of cycloadduct formation via geminate combination of triplet radical pairs.

Attempts to trap the intermediate triplet species with oxygen were unsuccessful. Irradiation of oxygen-saturated solutions led to no new NMR resonances, neither in the spectra taken after illumination nor in the CIDNP spectra, which are more sensitive than the former because the polarizations cause a large signal enhancement. Furthermore, no significant influence of oxygen on relative or absolute CIDNP signal intensities could be detected.

Triplet-Sensitization Experiments. To obtain information about photocycloadditions of ${}^3\mathbf{A} + \mathbf{FN}$ or ${}^3\mathbf{FN} + \mathbf{A}$, either or

both of these reactions necessarily being key steps in an electron-transfer/triplet mechanism such as has been inferred^{12,13} for systems similar to ours, we employed thioxanthone **TX** as triplet sensitizer to prepare ${}^3\mathbf{A}$ and ${}^3\mathbf{FN}$ indirectly, i.e., without intervention of radical ion pairs. Excitation of this sensitizer can be performed at $\lambda_{\text{exc}} \geq 390$ nm where none of the other compounds absorbs. **TX** possesses a triplet energy of 272 kJ mol⁻¹;⁴⁵ its reduction potential in acetonitrile vs SCE is -1.66 V.⁴⁶ Though being only weakly exergonic, energy transfer from ${}^3\mathbf{TX}$ is thus thermodynamically feasible for both anetholes as well as in the case of **FN** (Table 2). In contrast, electron transfer is seen to be endergonic by at least 20 kJ mol⁻¹.

A sample containing **TX**, 4×10^{-3} M of $t\mathbf{A}$, and 1×10^{-2} M of **FN** in acetonitrile-*d*₃ was illuminated, and the composition of the solution was monitored by NMR. We found that the photostationary equilibria between the geometric isomers of the substrate and those of the quencher were established fairly rapidly, pointing to efficient formation of both ${}^3\mathbf{A}$ and ${}^3\mathbf{FN}$. However, adducts **P1–P4** were nearly undetectable. This clearly shows that formation of a biradical from ${}^3\mathbf{A} + \mathbf{FN}$ or from ${}^3\mathbf{FN} + \mathbf{A}$ must be much less efficient than decay of these triplet molecules to their ground states, unless this biradical would almost entirely undergo cleavage after intersystem crossing instead of ring closure.

Discussion

Nature of the Additional Radical Pair. The findings reported in the preceding sections show that irradiation of our substrates in the absence of **FN** also leads to a radical pair, that one component of this pair is \mathbf{A}^+ and the other can only stem from the solvent and that its formation relies on a biphotonic process.

We interpret these experimental observations by two-photon ionization of the anetholes. Photoionization of these substrates by a biphotonic process is in accordance with expectations, since the ionization potential of $t\mathbf{A}$ in the gas phase is 7.83 eV;⁴⁷ despite the substantial reduction of the energy needed for ionization that is often found in fluid phase,⁴⁸ it is therefore unlikely that absorption of a single photon of wavelength 308 nm ($\cong 4.03$ eV) leads to emission of an electron. A recent laser flash-photolysis investigation also gave evidence for two-photon ionization of various other arylolefins.⁴⁴

The occurrence of nuclear spin polarizations in solutions of triethylamine in acetonitrile, when a charge-transfer band around 300 nm was excited with light of high intensity, has been reported, and these observations were explained by electron transfer from the amine to the solvent.⁴⁹ Likewise, the results of theoretical studies⁵⁰ as well as experimental investigations by pulse radiolysis⁵¹ point to a sufficient stability of the anion $\text{ACN}^{\bullet-}$ of acetonitrile or the dimeric species $(\text{ACN})_2^{\bullet-}$ to take part in formation of a radical ion pair. Finally, upon photolysis of 2,7-bis-(dimethylamino)-4,5,9,10-tetrahydropyrene in acetonitrile a transient absorption with a half-life of 9 ns was detected, which was attributed to an ion pair consisting of the radical cation of the pyrene derivative and $(\text{ACN})_2^{\bullet-}$.⁵² While definitive identification of the anion contained in the radical pairs that

(45) Dalton, J. C.; Montgomery, F. C. *J. Am. Chem. Soc.* **1974**, *96*, 6230–6232.

(46) Yates, S. F.; Schuster, G. B. *J. Org. Chem.* **1984**, *49*, 3349–3356.

(47) Caldwell, R. A.; Smith, L. *J. Am. Chem. Soc.* **1974**, *96*, 2994–2996.

(48) Lesclaux, R.; Jousset-Dubien, J. In *Organic Molecular Photophysics*; Birks, J. B., Ed.; Wiley: New York, 1973; Vol. 1, p 457.

(49) Bargon, J. in ref 14d, pp 393–398.

(50) Jordan, K. D.; Wendoloski, J. J. *Chem. Phys.* **1977**, *21*, 145–154.

(51) Bell, I. P.; Rodgers, M. A. J. *J. Chem. Soc., Faraday Trans. 1* **1977**, *73*, 315–326.

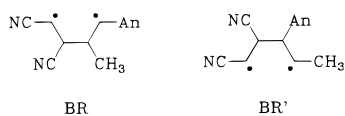
(41) Closs, G. L.; Sitzmann, E. V. *J. Am. Chem. Soc.* **1981**, *103*, 3217–3219.

(42) Zweig, A.; Hodgson, W. G.; Jura, W. H. *J. Am. Chem. Soc.* **1964**, *86*, 4124–4129.

(43) Eriksen, J.; Foote, C. S. *J. Am. Chem. Soc.* **1980**, *102*, 6083–6088.

(44) Johnston, L. J.; Schepp, N. P. *J. Am. Chem. Soc.* **1993**, *115*, 6564–6571.

Chart 1



are formed in the absence of **FN** in our systems cannot be drawn on the basis of our CIDNP experiments, and, besides, the actual nature of these pairs is unimportant for the mechanistic conclusions that follow, it thus seems very reasonable that the electron removed from the substrate is taken up by the solvent to give a monomeric or oligomeric anion $(\text{ACN})_x^{\bullet-}$. The *g* value of this radical anion $\text{X}^{\bullet-}$ is expected to be very similar to that of $\text{FN}^{\bullet-}$, i.e., lower than that of $\text{A}^{\bullet+}$, which is consistent with the fact that the CIDNP phases of the starting and the isomerized anethole are not influenced by the presence or absence of the quencher **FN**.

Pathway to the Cycloadducts. Owing to the configurational stability of the anethole radical cations, the radical ion pairs occurring in the systems *tA*/**FN** and *cA*/**FN** are chemically different species that cannot be interconverted during their life. Yet, in both cases the same cycloadducts are found, and the relative yields of their isomers **P1**–**P4** are also identical. This clearly shows that between the radical pairs and the adducts there must be a common intermediate, in which the stereochemical information of the olefin configuration is lost.

Even if a mechanism involving back electron transfer of $\text{A}^{\bullet+}\text{FN}^{\bullet-}$ to give either ^3A or ^3FN followed by cycloaddition in the triplet state operated, this loss could not be ascribed to isomerization at the stage of the triplet olefin, since intermediate formation neither of $^3\text{A} + \text{FN}$ nor of $\text{A} + ^3\text{FN}$ can account for the product distribution, which is characterized by complete one-way *cis*–*trans* isomerization of the anethole moiety; the first alternative would lead to bidirectional isomerization of this fragment and the second to retention of the configuration of the starting anethole. Hence, neither of these two triplet species qualifies as that key intermediate common to both our reaction systems which is responsible for the stereochemistry of the cycloadducts.

In contrast, the observed product distribution is perfectly consistent with formation of triplet biradicals and isomerization at this stage by rotations around single bonds. In principle, the two regioisomers ^3BR and $^3\text{BR}'$ displayed in Chart 1 could both explain the stereochemistry of the products. However, biradical $^3\text{BR}'$, which lacks the benzylic stabilization of one radical center, can be ruled out by thermodynamic arguments, as will be shown below.

A methyl substituent will only exhibit a negligible interaction with a vicinal cyano group. Furthermore, it is reasonable to assume that the precursors to the biradical approach in such a way that there is a small but nonzero angle between the molecular planes, thereby minimizing any repulsive orbital interactions involving the phenyl ring. The two diastereomers of ^3BR should therefore be formed in essentially equal amounts regardless of whether the configuration of the starting olefin is *cis* or *trans*. This is reflected by the fact that both with *cA* and with *tA* the yields of **P1** and **P4** are identical within experimental accuracy, as are those of **P2** and **P3**.

For 1,4-biradicals of similar constitution triplet lifetimes around 30 ns were determined.⁵³ Thus, it is reasonable to

assume^{6d,54} that complete equilibration of conformations takes place during the life of this open-chain compound. The fact that in all cycloadducts the anisyl group occupies a *trans* position with respect to the methyl substituent regardless of the configuration of the starting anethole, and the statistically distributed configuration of the sterically undemanding cyano substituent at C⁴ can be rationalized in this way. Analogous triplet biradicals were shown to occur as intermediates in Paterno–Büchi photocycloadditions of anetholes to quinones, which also proceed via radical ion pairs.¹⁷ In that case, equilibrium between the different conformers is not always established owing to the extremely short life of the Paterno–Büchi biradicals involved, and, consequently, the product distribution exhibits a temperature dependence. However, the products formed at high temperatures, where bond rotation is able to compete more favorably with intersystem crossing, likewise possess *trans* configurations of the anisyl and methyl groups independent of the stereochemistry of the starting anethole.

The different ratios of adduct polarizations to polarizations of the isomerized substrate that are found in the systems *tA*/**FN** and *cA*/**FN** further corroborate the intermediacy of such a triplet biradical. After intersystem crossing of substituted tetramethylene-1,4-biradicals, ring closure is frequently accompanied by homolytic scission of the 2,3-bond.^{54,55} Thus, in addition to bidirectional isomerization of the starting anethole via ^3A formed by back electron transfer of the radical ion pairs there should be an isomerization route via the triplet biradicals, which, however, leads to one-way *cis*–*trans* isomerization only.

If the probabilities of formation of ^3A from $^3\text{A}^{\bullet+}\text{FN}^{\bullet-}$ and $^3\text{cA}^{\bullet+}\text{FN}^{\bullet-}$ are similar, and if the same holds for the probabilities of biradical formation from these two pairs, which both seems reasonable to assume, the yield of isomerized substrate is therefore expected to be higher for the system *cA*/**FN** than in the case of *tA*/**FN**. This is indeed found, and manifests itself impressively by the approximately three times higher limiting value of the ratio μ_p/μ_{iso} at large quencher concentrations that is observed with *tA* as substrate (compare Figure 3).

We should like to point out that neither the absence of CIDNP in trapping products when the reactions are carried out in oxygen-saturated solutions nor the unchanged relative CIDNP intensities under these circumstances rule out the occurrence of triplet biradicals. It is known that Heisenberg spin exchange is an important, and perhaps even often a dominant, mechanism of oxygen quenching of biradicals.⁵⁶ This pathway would not lead to formation of new products bearing polarizations. Nor would it destroy polarizations since CIDNP generation is completed at the stage of the radical ion pairs; afterwards, the existing polarizations are only transferred to subsequent intermediates and finally to the end products. Significant effects could only result with this mechanism if the lifetime of ^3BR were reduced below about 1 ns such that equilibration of conformations were no longer possible; then, the product distribution and also the ratio μ_p/μ_{iso} would change. However, as a lifetime of some 20 ns is estimated⁵⁷ for the case that the biradical life were only limited by oxygen quenching, this seems unattainable under our experimental conditions.

(54) Schuster, D. I.; Heibel, G. E.; Woning, J. *Angew. Chem., Int. Ed. Engl.* **1991**, *30*, 1345–1347.

(55) (a) Lewis, F. D.; Hirsch, R. H. *J. Am. Chem. Soc.* **1976**, *98*, 5914–5924. (b) Wagner, P. J. *Acc. Chem. Res.* **1971**, *4*, 168–177. (c) Barton, D. H. R.; Charpiot, B.; Ingold, K. U.; Johnston, L. J.; Motherwell, W. B.; Scaiano, J. C.; Stanforth, S. *J. Am. Chem. Soc.* **1985**, *107*, 3607–3611.

(56) Caldwell, R. A.; Creed, D. *J. Am. Chem. Soc.* **1978**, *100*, 2905–2907.

(52) (a) Hirata, Y.; Mataga, N.; Sakata, Y.; Misumi, S. *J. Phys. Chem.* **1982**, *86*, 1508–1511. (b) Hirata, Y.; Takimoto, M.; Mataga, N. *Chem. Phys. Lett.* **1983**, *97*, 569–572. (c) Hirata, Y.; Mataga, N.; Sakata, Y.; Misumi, S. *J. Phys. Chem.* **1983**, *87*, 1493–1498.

(53) Kaprinidis, N. A.; Lem, G.; Courtney, S. H.; Schuster, D. I. *J. Am. Chem. Soc.* **1993**, *115*, 3324–3325.

The energy of ${}^3\text{BR}$ must lie below that of ${}^3\text{A} + \text{FN}$ or that of $\text{A} + {}^3\text{FN}$, because in all three instances the overall bond order is the same, but ${}^3\text{BR}$ possesses one additional σ -bond instead of a π -bond and the unfavorable interaction of the unpaired electrons is certainly lower in the 1,4-biradical than in the triplet of the donor or the acceptor olefin. A numerical value can be obtained by using Benson's⁵⁸ and Caldwell's⁵⁹ group increments. By this procedure,⁶⁰ we estimated ΔG^0 of ${}^3\text{BR}$ relative to $t\text{A} + \text{FN}$ to be $+197 \text{ kJ mol}^{-1}$, which is much lower than the triplet energies, in accordance with the above qualitative argument. On the other hand, formation of ${}^3\text{A}$ as well as of ${}^3\text{FN}$ from triplet pairs is thermodynamically feasible in our systems (compare Table 2) and indeed takes place, as is evidenced by the bidirectional isomerization of the substrates and the isomerization of the quencher FN . Hence, both direct reaction of ${}^3\text{A}^+\text{FN}^{\cdot-}$ to ${}^3\text{BR}$ and indirect formation of this triplet biradical from the radical ion pairs via the intermediacy of ${}^3\text{A}$ or ${}^3\text{FN}$ —the electron-transfer/triplet mechanism proposed for photocycloadditions of other donor and acceptor olefins^{12,13} or photodimerizations of olefins⁶¹—are conceivable. On the grounds of kinetic considerations, one might expect the indirect routes to be preferred because geminate combination of a radical ion pair to give a biradical requires cation and anion to be in actual contact and presumably to possess a favorable orientation, whereas back electron transfer of such a pair can occur at larger separations⁶² and probably needs weak orbital overlap only.

(57) The saturation concentration of oxygen in acetonitrile at room temperature is $9 \times 10^{-3} \text{ M}$ (Murov, S. L.; Carmichael, I.; Hug, G. L. *Handbook of Photochemistry*; Marcel Dekker: New York, 1993). A rate constant of $6 \times 10^9 \text{ M}^{-1} \text{ s}^{-1}$ was determined for O_2 quenching of a Norrish II 1,4-biradical (Small, R. D.; Scaiano, J. C. *J. Phys. Chem.* **1977**, *81*, 2126–2131). With these data, a first-order rate constant of $(19 \text{ ns})^{-1}$ is thus obtained.

(58) Benson, S. W.; Cruickshank, F. R.; Golden, D. M.; Haugen, G. R.; O'Neal, H. E.; Rodgers, A. S.; Shaw, R.; Walsh, R. *Chem. Rev.* **1969**, *69*, 279–324.

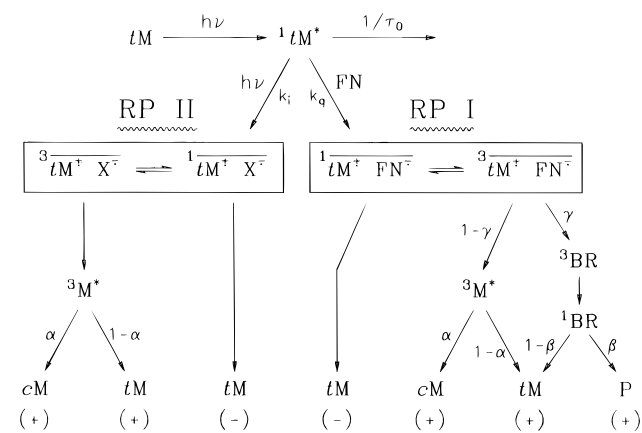
(59) Ni, Tuqiang; Caldwell, R. A.; Melton, L. A. *J. Am. Chem. Soc.* **1989**, *111*, 457–464.

(60) We use Benson's nomenclature⁵⁸ of groups in the following. Increments for nonradical groups are from ref 58, for radical groups from ref 59. According to ref 59, olefin triplets may be regarded as 1,2-biradicals to a very good approximation and described by the same group increments as 1,4-biradicals. For calculation of ΔH^0 of the quencher-based moiety in ${}^3\text{BR}$ we therefore take half the triplet energy of FN , which corresponds to replacing one group $\text{C}_d(\text{H})(\text{CN})$ by $\cdot\text{C}(\text{H})(\text{C})(\text{CN})$. To take into account the combination with the anethole fragment, we subtract from this the increment for $\text{C}(\text{C}_T)(\text{C}_2)(\text{H})$, $+28 \text{ kJ mol}^{-1}$, and add the increment for $\text{C}_d(\text{C}_T)(\text{H})$, -7 kJ mol^{-1} . The result is $+95 \text{ kJ mol}^{-1}$. Likewise, the triplet energy of the anethole may be thought of as arising from converting $\text{C}_d(\text{C}_B)(\text{H})$ into $\cdot\text{C}(\text{C}_B)(\text{C})(\text{H})$, and $\text{C}_d(\text{H})(\text{C})$ into $\cdot\text{C}(\text{C}_2)(\text{H})$. The former change also occurs in the transformation from $t\text{A}$ to ${}^3\text{BR}$; furthermore, in going from ${}^3\text{A}$ to ${}^3\text{BR}$ the group $\cdot\text{C}(\text{C}_2)(\text{H})$ (increment $+172 \text{ kJ mol}^{-1}$) must be replaced by $\text{C}(\text{H})(\text{C}_3)$ (increment -8 kJ mol^{-1}). This puts ΔH^0 of this fragment at $+70 \text{ kJ mol}^{-1}$. The total value of ΔH^0 of the biradical relative to the value for the starting materials is therefore $+165 \text{ kJ mol}^{-1}$. The predominant contribution to ΔS^0 is the change of one olefinic carbon atom in $t\text{A}$ and one in FN into two aliphatic carbon atoms in ${}^3\text{BR}$. For the anethole part we must therefore subtract the increment for $\text{C}_d(\text{H})(\text{C})$, $+33 \text{ J K}^{-1} \text{ mol}^{-1}$, and add the increment for $\text{C}(\text{H})(\text{C}_3)$, $-51 \text{ J K}^{-1} \text{ mol}^{-1}$; for the quencher-based moiety we must subtract the increment for $\text{C}_d(\text{C}_d)(\text{H})$, $+27 \text{ J K}^{-1} \text{ mol}^{-1}$, and add the increment for $\text{C}(\text{C}_3)(\text{C}_2)(\text{H})$, $-47 \text{ J K}^{-1} \text{ mol}^{-1}$. However, this overestimates the decrease in entropy occurring in combination to the biradical, since it does not take into account the conformational flexibility introduced by the transformation of the two other olefinic carbon atoms into two radical centers. To correct for this effect, we need the increment for ΔS^0 of the group $\cdot\text{C}(\text{C}_2)(\text{H})$, which we estimate to be $+58 \text{ J K}^{-1} \text{ mol}^{-1}$ by subtracting twice the increment for $\text{C}(\text{H}_3)(\text{C})$, $+116 \text{ J K}^{-1} \text{ mol}^{-1}$, from the experimental value of ΔS^0 for *iso*- C_3H_7 , $+290 \text{ J K}^{-1} \text{ mol}^{-1}$ (Tsang, W. *J. Am. Chem. Soc.* **1985**, *107*, 2872–2880). As the increment for an olefinic group $\text{C}_d(\text{H})(\text{C})$ is $+33 \text{ J K}^{-1} \text{ mol}^{-1}$, we thus get a total value of ΔS^0 for formation of the biradical from $t\text{A} + \text{FN}$ of $-108 \text{ J K}^{-1} \text{ mol}^{-1}$. Hence, at room temperature the entropy contribution to ΔG^0 is about 20% of the enthalpy contribution.

(61) Farid, S.; Brown, K. A. *J. Chem. Soc., Chem. Commun.* **1976**, 564–565.

(62) Rehm, D.; Weller, A. *Isr. J. Chem.* **1970**, *8*, 259–271.

Scheme 1



However, the fact that the yields of cycloadducts from the radical ion pairs neither depend on the quencher concentration (see Figure 4) nor on the concentration of the substrate (Figure 5) cannot be reconciled with biradical formation by attack of ${}^3\text{A}$ to FN or by attack of ${}^3\text{FN}$ to A . Further corroboration is obtained by the triplet sensitization studies, where both ${}^3\text{A}$ and ${}^3\text{FN}$ are generated as is seen from the attainment of the photostationary equilibria between the *cis*- and *trans*-forms of both substrate and quencher, but where the cycloadduct yields are negligible; as the biradical has been established as precursor to P1 to P4 by the stereochemical arguments given above, this observation must be ascribed to a very low yield of ${}^3\text{BR}$ from ${}^3\text{A} + \text{FN}$ as well as from ${}^3\text{FN} + \text{A}$. Hence, these findings rule out a significant contribution of the indirect route, triplet radical ion pair \rightarrow olefin triplet \rightarrow triplet biradical, to cycloaddition in our systems; instead, the biradicals must be formed directly, by geminate combination of radical ion pairs in triplet states. This direct pathway is also consistent with the results of our studies of photocycloadditions of anetholes to quinones.¹⁷ In these reactions, neither ${}^3\text{A}$ nor triplet quinones can be formed for energetic reasons, yet efficient adduct formation takes place by the direct route.

Finally, ΔG^0 of the regioisomer ${}^3\text{BR}'$ can be calculated as above by using group increments. It is found⁶³ that the free enthalpy of ${}^3\text{BR}'$ ($+257 \text{ kJ mol}^{-1}$ relative to $t\text{A} + \text{FN}$) is higher by 60 kJ mol^{-1} than that of ${}^3\text{BR}$. This is of course a manifestation of the difference in stabilization of a benzyl radical and a secondary alkyl radical. Comparison with the data of Table 2 shows that formation of ${}^3\text{BR}$ from the radical ion pairs ${}^3\text{A}^+\text{FN}^{\cdot-}$ is exergonic by some 60 kJ mol^{-1} , whereas the driving force for formation of ${}^3\text{BR}'$ is practically zero. By these thermodynamic considerations, a participation of ${}^3\text{BR}'$ in our reactions is seen to be very unlikely. ${}^3\text{BR}$ is also kinetically favored over ${}^3\text{BR}'$: Our AM1 computations of $\text{A}^{\cdot+}$ gave the highest positive charge density at the β carbon atom; it is thus reasonable that combination with $\text{FN}^{\cdot-}$ takes place at this position, which leads to ${}^3\text{BR}$.

Reaction Mechanism and Determination of Parameters.

All our experimental findings are explained by the reaction mechanism given in Scheme 1. For simplicity, this Scheme has been drawn for the system $t\text{A}/\text{FN}$ only. An analogous scheme results when the starting anethole is $c\text{A}$. The signs given at the final products indicate the polarization phases of their

(63) The difference in ΔG^0 for ${}^3\text{BR}$ and ${}^3\text{BR}'$ should be solely determined by the difference in ΔH^0 . In the transformation ${}^3\text{BR} \rightarrow {}^3\text{BR}'$, the groups $\cdot\text{C}(\text{C}_B)(\text{C})(\text{H})$ (increment $+116 \text{ kJ mol}^{-1}$)⁵⁹ and $\text{C}(\text{C}_3)(\text{H})$ (-8 kJ mol^{-1})⁵⁸ change into $\text{C}(\text{C}_B)(\text{C}_2)(\text{H})$ (-4 kJ mol^{-1})⁵⁸ and $\cdot\text{C}(\text{C}_2)(\text{H})$ ($+172 \text{ kJ mol}^{-1}$),⁵⁹ respectively. ΔH^0 of ${}^3\text{BR}'$ is thus more positive than ΔH^0 of ${}^3\text{BR}$ by 60 kJ mol^{-1} .

methyl protons; these phases depend on the respective pathway of product formation.

The excited substrate decays with its unquenched life τ_0 to the educt anethole and to a small degree also to the isomerized anethole and to a dimer, all of which bear no polarizations and have therefore been omitted from the scheme. $^1t\mathbf{A}$ is quenched by \mathbf{FN} to give a pair $t\mathbf{A}^{+\bullet}\mathbf{FN}^{\bullet-}$ (RP I) with rate constant k_q and reacts to a radical pair $t\mathbf{A}^{+\bullet}\mathbf{X}^{\bullet-}$ (RP II) in a biphotonic process with rate constant k_i . Both pairs originate in the singlet state.

In the radical ion pairs, intersystem crossing takes place. Owing to the higher g value of the anethole radical cation compared to that of $\mathbf{X}^{\bullet-}$ or $\mathbf{FN}^{\bullet-}$ and because the hyperfine coupling constant of the methyl protons in $\mathbf{A}^{+\bullet}$ is positive, intersystem crossing of these pairs is the faster the higher (i.e., more positive) the z projection of the particle spin of the methyl group. In consequence, both in the case of RP I and in that of RP II absorptive nuclear spin polarizations of the methyl protons develop in the triplet pairs and emissive polarizations in the singlet pairs.

As has been shown, escape from the cage plays no role with respect to CIDNP in these systems except in time-resolved measurements. By reverse, as far as steady-state polarizations are concerned the singlet pairs of RP I and RP II can be thought of as decaying exclusively by back electron transfer (compare also note 64), thereby transferring their emissive polarizations to the regained substrate. Back electron transfer of triplet pairs to give $^3\mathbf{A}$ is also possible for RP I as well as RP II. Decay of this phantom triplet leads to $c\mathbf{A}$ and $t\mathbf{A}$ with efficiencies α and $1 - \alpha$, so the absorptive polarizations transferred to $^3\mathbf{A}$ from both pairs are partitioned between the starting and the isomerized anethole.

In the same manner, back electron transfer of $^3t\mathbf{A}^{+\bullet}\mathbf{FN}^{\bullet-}$ to give $^3\mathbf{FN} + \mathbf{A}$ occurs, as is evidenced by the polarizations of the isomerized quencher \mathbf{MN} (see Figure 1). One could thus hope to obtain the relative yields of $^3\mathbf{A}$ and $^3\mathbf{FN}$ from the CIDNP spectra. While in principle this is indeed possible, in our experiments the reproducibility of the polarization intensities of \mathbf{FN} and \mathbf{MN} was too poor to permit such a quantitative evaluation. We attribute this to protonation of these radical anions by traces of water present in varying amount in the samples. For clarity, this reaction has therefore been omitted from Scheme 1. Its neglect does not influence the relative polarizations of the anethole species and the anethole derived moieties in the products.⁶⁴

Besides back electron transfer, geminate reaction to give a triplet biradical $^3\mathbf{BR}$ provides an additional decay pathway of $^3t\mathbf{A}^{+\bullet}\mathbf{FN}^{\bullet-}$. We assign an efficiency γ to biradical formation, and an efficiency $1 - \gamma$ to formation of the triplet anethole from this pair, thereby referring both processes to unit efficiency of formation of a species other than $^3\mathbf{FN}$. Regardless of the rate of the reaction $^3\mathbf{RP I} \rightarrow ^3\mathbf{FN} + t\mathbf{A}$, the ratio of rate constants for the processes $^3\mathbf{RP I} \rightarrow ^3\mathbf{BR}$ and $^3\mathbf{RP I} \rightarrow ^3\mathbf{A} + \mathbf{FN}$ is thus given by $\gamma/(1 - \gamma)$. At the stage of the biradical, equilibration of conformations occurs. Finally, after intersystem crossing to the singlet state, ring closure of $^1\mathbf{BR}$ (efficiency β) leads to the

cycloadducts, whereas biradical cleavage (efficiency $1 - \beta$) produces $t\mathbf{A}$ only.

On the basis of this mechanism, the dependence of the polarization ratio μ_p/μ_{iso} on quencher concentration (Figure 3) and light intensity (Figure 6) can be rationalized with changes in the yields of the intermediates RP I and RP II, which are formed by competitive processes; to some degree, transformations of RP II into RP I by interception of $\mathbf{X}^{\bullet-}$ with \mathbf{FN} must also be taken into account. A quantitative description of the chemical kinetics up to and including the radical pairs as well as of the scavenging experiments will be given in a forthcoming publication.⁶⁵ The present work, apart from elucidation of the general reaction mechanism, mainly focuses on geometric isomerization and cycloaddition, i.e., processes occurring *after* the stage of the radical ion pairs. Kinetic information about these steps can be obtained from the CIDNP measurements at high quencher concentrations, where $^1\mathbf{A}$ is essentially deactivated by quenching with \mathbf{FN} only, and where the role of RP II is thus negligible.

With the starting anethole being $t\mathbf{A}$, it is obvious from Scheme 1 that the ratio of adduct polarizations to polarizations of the isomerized substrate in the limit of infinite quencher concentration, $(\mu_p/\mu_{iso})_{t\mathbf{A}}^{\text{lim}}$, is

$$\left(\frac{\mu_p}{\mu_{iso}}\right)_{t\mathbf{A}}^{\text{lim}} = \frac{\beta\gamma}{\alpha(1 - \gamma)} \quad (4)$$

Setting up the reaction scheme for $c\mathbf{A}$ as starting anethole, we arrive at the corresponding quantity $(\mu_p/\mu_{iso})_{c\mathbf{A}}^{\text{lim}}$

$$\left(\frac{\mu_p}{\mu_{iso}}\right)_{c\mathbf{A}}^{\text{lim}} = \frac{\beta\gamma'}{(1 - \beta)\gamma' + (1 - \alpha)(1 - \gamma')} \quad (5)$$

where α and β by necessity are the same parameters as in the system $t\mathbf{A}/\mathbf{FN}$, but where the efficiency γ' of biradical formation might differ from γ . However, it seems reasonable to assume that γ and γ' are identical, since the driving force for back electron transfer of $^3\mathbf{RP I}$ to give \mathbf{FN} plus the respective triplet anethol is very similar in both cases (compare Table 2), the same holds for the driving force of biradical formation, and an influence of the configuration of the anethole cation on the rate of biradical formation is not to be expected. The parameter α is 0.59, as was determined from the photostationary state reached in the benzophenone-sensitized isomerization of anethole;⁶⁶ α depends only on the potential curves of anethole in the ground state and in the triplet state, it should be constant within the range of temperatures encountered in our experiments. With this value, and on the assumption that γ and γ' are equal, β and γ can be obtained in a straightforward way from the observed polarization ratios in the limit of high quencher concentration, by using eqs 4 and 5. Error analysis shows that β and γ are only weak functions of the polarization ratios, so the accuracy (an estimated 1%) is not severely affected by possible small deviations of the experimental values of μ_p/μ_{iso} from the limiting values nor by fluctuations of the data.

The efficiency of biradical formation γ is found to be fairly large, between 0.69 at 312 K and 0.73 at 241 K, so geminate reaction of $^3\mathbf{RP I}$ to the biradical $^3\mathbf{BR}$ is faster than back electron transfer to give $^3\mathbf{A}$ by a factor of more than 2. Since only relative rate constants can be obtained from these measurements, it is not immediately clear whether back electron transfer is rather slow or biradical formation unusually fast in these systems. However, a comparatively low rate of back electron

(64) If a fraction δ of $^3t\mathbf{A}^{+\bullet}\mathbf{FN}^{\bullet-}$ reacts to $^3\mathbf{FN} + t\mathbf{A}$, this fraction of the polarizations is transferred from $t\mathbf{A}^{+\bullet}$ in the triplet pairs to the starting anethole, hence the opposite polarizations in this compound resulting from the singlet exit channel are decreased by δ . Exactly the same fraction of the polarizations from the triplet exit channel is missing in $^3\mathbf{A}$ and $^3\mathbf{BR}$ and all their subsequent products. In evaluations of relative polarizations stemming from the anethole radical cation only, this reaction is thus unimportant. The same argument can be used to explain why omission of escaping radical ions does not influence relative polarizations as long as no relaxation losses occur.

(65) Eckert, G.; Goez, M. Manuscript in preparation.

(66) Caldwell, R. A.; Pac, C. *Chem. Phys. Lett.* **1979**, *64*, 303–306.

transfer is made plausible by the low driving force of this process, $-\Delta G^0$ of it being 10–12 kJ mol⁻¹ only. According to the above calculations of the thermodynamics of ³BR, $-\Delta G^0$ for biradical formation is more than five times higher than this. The fact that for spin-allowed electron transfer the critical reaction distance is larger than for bond formation⁶² is thus obviously outweighed by these thermodynamic aspects. In contrast, singlet pairs preferentially decay by back electron transfer, which is strongly exergonic in this case.

The experimentally determined efficiencies β for ring closure of ¹BR lie between 0.41 and 0.42 in the temperature interval considered. This agrees well with the values obtained in the photoreactions of various cycloalkanones with cyanosubstituted olefins,^{6d,54} which were all reported to fall into the range of 0.2–0.5.

The parameter γ is seen to decrease slightly when the temperature is raised. This appears reasonable, because higher temperatures should favor formation of two molecules over formation of a single species, i.e., favor back electron transfer to triplet species over combination of two radical ions to give a biradical. However, the same argument should also apply to cleavage of ¹BR, so one would expect a similar decrease of β with increasing temperature, which is not found experimentally. Instead, that parameter shows a very small rise with rising temperature. From a plot of the logarithm of $\gamma/(1 - \gamma)$ versus $1/T$ one can conclude that the activation enthalpy of back electron transfer to give ³A must be marginally larger than the activation enthalpy of biradical formation.

Finally, the noticeably different temperature dependence of the polarization ratios $(\mu_P/\mu_{iso})^{lim}$ in the systems *cA*/FN and *tA*/FN (compare Figure 7) is easily rationalized with the mechanism of Scheme 1. For these limiting polarizations RP II plays a negligible role. In both cases, cycloaddition relies on formation of ³BR and on ring closure of ¹BR, both processes having opposite temperature coefficients. The decrease in γ by some 5% in the experimental temperature interval is partly cancelled by the smaller increase in β (some 3% in that range), so the product $\beta\gamma$ varies only very little with *T*. In contrast, with regard to isomerization the two systems behave differently. With *tA* as starting olefin, isomerization solely occurs via back electron transfer to give ³A, the relative contribution of this decay pathway of RP I increasing with increasing temperature; to first approximation, this leads to a temperature dependence of $(\mu_P/\mu_{iso})_{tA}^{lim}$ that is given by $(1 - \gamma)^{-1}$. However, the system *cA*/FN possesses an additional isomerization pathway, via the biradical, so desactivation of RP I by either channel leads to a species capable of isomerization. The temperature dependence of $(\mu_P/\mu_{iso})_{cA}^{lim}$ is thus determined by the partitioning of RP I between these two pathways, which to first order possess similar isomerization efficiencies, $1 - \alpha$ and $1 - \beta$ being within 30% of each other. The remaining imbalance of these two channels is only a second-order effect. Indeed, by rewriting eq 5 and setting γ' equal to γ one arrives at

$$\left(\frac{\mu_P}{\mu_{iso}}\right)_{cA}^{lim} = \frac{\beta\gamma}{(1 - \alpha) + (\alpha - \beta)\gamma} \quad (6)$$

The numerator of this equation is almost temperature-independent, as explained above, and the constant first term in the denominator is much larger than the temperature-dependent second term.

Conclusions

Based on the results of our photophysical and photochemical experiments, especially the CIDNP measurements, we regard

it as established that in polar solvents basically the same mechanism governs the [2 + 2] cycloadditions of photoexcited donor olefins (anetholes) to acceptor olefins (fumarodinitrile) studied in the present work and the Paterno–Büchi reactions of photoexcited electron-deficient carbonyl compounds (quinones) with donor olefins (anetholes) investigated previously.¹⁷

In both cases, the first chemical step is full charge transfer to give radical ion pairs; we could unambiguously exclude pathways bypassing these pairs, as for instance cycloadditions via exciplexes, and could show that the pathways giving rise to CIDNP are the main reaction routes. At the stage of the radical ion pairs, intersystem crossing occurs. Singlet pairs decay by back electron transfer; triplet pairs do likewise if this is energetically feasible, e.g., in the anethole/fumarodinitrile systems. The latter process leads to the triplet of one or both reaction partners and thus provides a pathway to olefin isomerization; for olefins such as those employed in this work, this results in bidirectional isomerization.

The triplet pairs possess an important additional decay channel, namely geminate combination to give triplet biradicals. Indirect formation of these key intermediates, via back electron transfer of triplet pairs to give one of the reactants in the triplet state followed by attack to ground state molecules,^{12,13} is precluded by thermodynamics in the Paterno–Büchi systems studied.¹⁷ For the cycloadditions investigated in the present work, these indirect pathways would be thermodynamically feasible, and olefin triplets are indeed formed in the anethole/fumarodinitrile systems. Yet they do not lead to cycloaddition; our experimental findings clearly show that only the direct route to the biradical is taken.

Since the biradical is produced by combination of radical ions bearing opposite charges, it is initially formed with a geometry that is determined by maximum Coulomb stabilization of the precursor complex, hence a sandwich-like structure of the transition state.¹⁷ Whether or not the resulting biradical conformation—which will usually be energetically unfavorable, because a sandwich-type precursor with maximum area of contact between the radical ions preferentially leads to *anti* conformation of substituents in 1,4- and 2,3-positions—is preserved is decided by the competition between thermally actuated bond rotation in this open-chain compound and temperature-independent intersystem crossing. If intersystem crossing is much faster than bond rotation, as in Paterno–Büchi biradicals at low temperatures, the stereochemistry of the cycloadducts reflects the initial stereochemistry of the biradical. In that case, the reaction can lead to a single product; a different stereoisomer is obtained when the configuration of the educt olefin is changed. If the triplet life of the biradical is comparatively long, as in the systems of the present work, complete equilibration of conformations occurs, and several products result, the stereochemistry of which does not depend on the geometry of the starting olefin.

Finally, ring closure of the singlet biradical is accompanied by biradical cleavage. In the reactions of anetholes with both fumarodinitrile and with quinones, this provides an important pathway to unidirectional *cis*–*trans* isomerization of the substrate, which should be important in the cycloadditions of other aryl-substituted olefins as well.

It seems reasonable to assume that the mechanism of ionic photocycloaddition found for the Paterno–Büchi reactions of quinones with anetholes¹⁷ and for the [2 + 2] cycloadditions of the present work applies also to related reactions of donor and acceptor olefins in polar media. The following two features of this mechanism may be of interest for synthetic applications. First, if such ionic cycloadditions proceed via short-lived

biradicals and are carried out at low temperatures, they may lead to adducts possessing a stereochemistry that is decided by the Coulomb interactions in the transition state leading from the radical ion pair to the biradical. This may be exploited to obtain stereoisomers that are different from those resulting from nonionic cycloadditions of the same substrates and presumably are the sterically more demanding isomers in many cases. Second, the basic reaction mechanism is independent of the multiplicity of the excited species because intersystem crossing to the triplet state can also occur at the stage of the radical ion pairs. Hence, reactants can be employed that carry neither carbonyl functions nor other substituents enhancing the efficiency of intersystem crossing in the primary excited molecules. This should broaden considerably the range of compounds useable for these cycloadditions and could thus increase the synthetic potential of these reactions.

Experimental Section

Chemical Substances. *trans*-Anethole, *tA*, was doubly distilled in vacuum, fumarodinitrile, **FN**, 9-cyanoanthracene, **CNA**, and thioxanthone were purified by repeated sublimation at 10^{-6} bar, 1,2,4-trimethoxybenzene (97%) was used as received, and *cis*-anethole, *cA*, was prepared by bromination of the *trans*-isomer followed by dehydrohalogenation⁶⁷ and finally partial hydrogenation with a poisoned nickel catalyst under atmospheric pressure.⁶⁸ Spinning band column distillation gave a product containing about 5% of the *trans*-isomer. As the extinction coefficients of *tA* at the excitation wavelength is about a factor of 10 higher than that of *cA*, further purification was essential. This was done by GC (carbowax, column length 3 m, 180 °C, carrier H₂, solvent pentane), yielding a product with a purity of 99.6% (GC).

For the synthesis of the cycloadducts **P1–P4** by photoinduced electron transfer sensitization, 180 mg of *tA*, 380 mg of **FN**, and 15 mg of **CNA** were solved in 50 mL of acetonitrile. The solution was irradiated under nitrogen at $\lambda_{\text{exc}} > 385$ nm for several hours in a quartz vessel. After removal of the solvent in vacuum, the residue was fractionated by chromatography (ca. 30 cm SiO₂, cyclohexane/ethylacetate, 1:1), the eluate being monitored by NMR. The early (fluorescent) fractions consisted of *tA* and the homodimer ($\alpha,\beta,\alpha,\beta$)-1,2-dianisyl-3,4-dimethylcyclobutane, **D1**. The ¹H-NMR parameters (CD₃CN) of the latter are δ 1.131 (CH₃, m), δ 1.170 (H³, H⁴, m), δ 2.776 (H¹, H², m), δ 3.726 (OCH₃, s), δ 6.822 (Ph, m), δ 7.138 (Ph, m). The following two fractions contained **P1** plus **P2** and **P3** plus **P4**, respectively. By chromatography (SiO₂, CHCl₃) of these fractions, all four stereoisomers were finally obtained in sufficient purity and with yields of a few milligrams each. Their spectral parameters are given in Table 4.

(67) Fahey, R. C.; Schneider, H. J. *J. Am. Chem. Soc.* **1968**, *90*, 4429–4434.

(68) Davies, D. E.; Gilchrist, T. L.; Roberts, T. G. *J. Chem. Soc., Perkin Trans. I* **1983**, 1275–1281.

Sample Preparation. Acetonitrile-*d*₃ (ICB, 99.5% D) was dried over 3 Å molecular sieve prior to use. Except for the measurements with varying concentrations of *tA*, sensitizer concentrations of the CIDNP experiments were chosen such as to give an absorbance of the samples at the excitation wavelength of approximately 1. Directly after preparation, the samples were deoxygenated by bubbling purified nitrogen through the solutions, and then they were immediately sealed.

Photophysical, Stern–Volmer, and Potential Measurements. The lifetime of ¹*tA* in acetonitrile was determined with a time-correlated single-photon-counting apparatus that is described elsewhere.⁶⁹ Fluorescence measurements were carried out with a Perkin Elmer MPF-44 fluorescence spectrometer. The reduction potential of *tA* in acetonitrile was determined with a Metrohm 506 polarograph (supporting electrolyte, 0.1 M tetrabutylammonium hexafluorophosphate) against ferrocene/ferrocenium.

NMR and CIDNP Measurements. The NOE experiments of **P3** were performed with a Bruker AM-400 NMR spectrometer. For all other ¹H-NMR and CIDNP measurements, a Bruker WM-250 console was used. For data acquisition and experimental control the apparatus was interfaced to an 80486-based multitasking workstation equipped with a Keithley AD-converter and connected to a home-made programmable pulse generator. Illumination was done by an excimer laser, which was triggered by the pulse generator. A special probe allowed side-on illumination of the samples.^{70,71} Typically, 10% of the laser energy was absorbed in the samples, as determined actinometrically. The pulse sequences employed for the pseudo steady-state CIDNP measurements have been described previously.³³ This technique leads to strong suppression of background signals, and the CIDNP intensities are practically undisturbed by nuclear-spin relaxation in the diamagnetic products.

Calculations. Force-field calculations were performed with the program PC MODEL (version 4.0)⁷² on a personal computer, and AM1⁷³ calculations with MOPAC 5.0 package were run on an IBM 3090 mainframe computer.

Acknowledgment. Financial support by the Deutsche Forschungsgemeinschaft is gratefully acknowledged. We are indebted to the following members of the Technische Universität Braunschweig, the respective institute given in parentheses: to J. Küster (Physical Chemistry) for determining the singlet lifetime of *tA* in acetonitrile; to A. Plagens (Organic Chemistry) for his help in the GC purification of *cA*; and to Mrs. P. Schulz (Organic Chemistry) for carrying out the 400 MHz NOE measurements on compound **P3**.

JA9511578

(69) Dreeskamp, H.; Salthammer, T.; Läufer, A. *J. Lumin.* **1989**, *44*, 161–165.

(70) Läufer, M.; Dreeskamp, H. *J. Magn. Reson.* **1984**, *60*, 357–365.

(71) Goez, M. *Chem. Phys.* **1990**, *147*, 143–154.

(72) Serena Software, Bloomington, 1990.

(73) Dewar, M. J. S.; Zoebisch, E. G.; Healy, E. F.; Stewart, J. J. P. *J. Am. Chem. Soc.* **1985**, *107*, 3902–3909.